Who Pays the Bill? Climate Change, Taxes, and Transfers in a Multi-Region Growth Model[*]

Elmar Hillebrand[†]   Marten Hillebrand[‡]

November 2, 2021

Abstract

This paper presents a quantitative study of a dynamic climate-economy model with multiple regions to evaluate how implementing an optimal climate tax affects production, emissions, and welfare in each region. We develop a numerical algorithm which is generally applicable to compute equilibria in the presence of arbitrarily many regions and under alternative climate policies. Our simulation model distinguishes six major world regions and incorporates a wide array of regional heterogeneities including a detailed description of the energy production process in each region. We also quantify the full range of Pareto-improving transfers under which each region has an incentive to join the global climate agreement. Our results show that optimal taxation reduces coal consumption in each region substantially by about 70% and leads to higher GDP within the next 100 years in most regions. The only exception is China which suffers losses in GDP for the next 130 years due to its strong dependence on coal and must be incentivized via transfer payments to implement the optimal tax. We also show that the increase in global temperature under optimal taxation is compatible with the two-degree target.

JEL classification: C63, E61, H21, H23, Q54

Keywords: Climate Change; Multi-region dynamic general equilibrium model; Optimal climate policy; Pareto-improving transfer payments; Cumulative adjustment costs; Two-degree target.

Introduction

There is now a broad consensus that emissions from burning fossil fuels are the main driver of climate change and must be reduced substantially, immediately, and permanently. Since this is a global problem, it can only be solved by a global climate agreement in which all major world regions coordinate on a joint climate policy with explicit and binding emissions targets. Reaching such an agreement is difficult, however, since world regions differ substantially along many dimensions such as their state of economic development, projected climate damages, or dependence on but also reserves of fossil fuels, which is a major source of income notably in oil-exporting countries. Hence, each region has different incentives to implement a joint climate policy.

From an economic standpoint, understanding the economic consequences and the costs and benefits of climate policies at the regional level and incorporating these insights into a common policy proposal is therefore key for the success of any climate agreement. This requires a theoretical framework which incorporates the key sources of regional heterogeneity and permits to quantify the consequences of climate policy at the regional level. Such a quantitative study is the general contribution of the present paper. Our simulation model distinguishes six major world regions which played a major role in past climate agreements such as the 2015 Paris accord. These include the United States, China, and Europe which are responsible for most emissions as well as poor and developing regions which are most affected by climate damages. We also incorporate many sources of regional heterogeneity and a detailed description of energy production based on clean and dirty technologies and different types of fossil fuels.

Our study consists of three parts. First, we evaluate the effects of implementing an optimal global emissions tax on key economic variables in each region. This includes the gains and losses in aggregate production output but also the structural transformations in regional energy production and the induced changes in emissions. Such an evaluation permits to measure the total costs that each region incurs by joining the global climate agreement and to evaluate its economic consequences at various levels.

Second, we quantify the complete range of transfer payments under which each region benefits from the climate agreement. This result permits to complement the global climate tax by a transfer scheme which redistributes tax revenue such that each region has an incentive to join the climate agreement. By aggregating the minimal transfers received by each region, we also obtain an estimate of the global funds that could be channeled to developing regions in order to support their efforts to build 'clean, climate-resilient futures' as stated in the Paris agreement (cf. UNFCCC (2015)).

Third, to obtain reliable predictions, we provide a thorough calibration of each region's economic characteristics drawing on a variety of empirical sources including detailed energy production data. To further substantiate our findings, we perform a series of careful robustness checks on key model parameters and discuss the consequences of

alternative specifications along with an evaluation of the backward consistency of the employed climate model. These results constitute the final part of our study.

Our paper contributes to a large and growing literature which analyzes the climate problem using so-called Integrated-Assessment models. These models incorporate the full interactions between the macroeconomy and the climate system. Modern incarnations of this class are based on the dynamic general equilibrium paradigm which is the standard modeling device in modern macroeconomics. Examples are Golosov et al. (2014) (henceforth GHKT), who derive an optimal climate tax policy in closed form, Rezai & van der Ploeg (2015) who study how the GHKT-result changes under more general preferences and technologies, Gerlagh & Liski (2018) who include hyperbolic discounting and an alternative climate model, or Barrage (2020) who explores how fiscal distortions affect the optimal climate policy. All these studies treat the world as a single region which abstracts from the importance of regional heterogeneities discussed above. Hassler & Krusell (2012) extend the GHKT-model to a multi-region framework in which oil-exporting and -importing regions trade on a global oil-market. Hassler et al. (2020) extend this model further to incorporate multiple energy sources and conduct a numerical study in the same spirit as we do in this paper.

We build upon the multi-region framework and theoretical results from Hillebrand & Hillebrand (2019). In this earlier paper, we used a parsimonious numerical example with only two regions and two energy sources to illustrate our results. Our main contribution relative to Hillebrand & Hillebrand (2019) is a comprehensive quantitative evaluation of optimal climate polices based on a much larger set of realistically calibrated regions chosen to represent the major players in past climate negotiations. In addition, our simulation model distinguishes multiple energy sources calibrated to match a variety of empirical features. This allows us to obtain quantitative results on the substitution between different clean and dirty technologies for each region and the transition to a clean economy. Our calibration strategy determines an explicit mapping from a rich set of calibration targets comprising key global and regional features to the model parameters. This sets the stage for addressing the political issues motivated above.

We also extend the theoretical scope of the analysis in Hillebrand & Hillebrand (2019) by including an alternative policy scenario where regions do not cooperate and instead choose regionally optimal taxes to internalize domestic climate damages. This non-cooperative tax policy can also be derived in closed form (cf. Hillebrand & Hillebrand (2021)) and we provide a quantitative assessment of it in our simulation study. This complements recent findings by Hambel et al. (2021) who also determine the non-cooperative equilibrium in a model with regionally differentiated commodities and a climate model based on the DICE-framework (Nordhaus & Sztorc (2013)). Similar to the standard DICE-model, Hambel et al. (2021) do not model the energy production stage and climate policy corresponds to choosing an abstract emissions control rate.

A key difference of our model to Hassler & Krusell (2012) and Hassler et al. (2020) is

that we allow for additional channels of trade and borrowing and lending between regions via an international capital market. This assumption is key to obtain an optimal climate tax policy in closed form which may be viewed as a multi-region extension of the GHKT-model. We discuss the advantages and limits of our theoretical framework in Section 5.

An alternative class of models is based on the DICE framework developed by Nordhaus (1991) and further detailed in Nordhaus & Boyer (2000). The model is extended to a multi-region framework in Nordhaus & Yang (1996), the so-called RICE-model. Both models have been highly influential for our quantitative economic understanding of climate change and form the basis for numerous studies in the literature, including many large-scale integrated assessment models such as MERGE, REMIND, or WITCH. There is also a large literature which studies optimal transfers in international climate agreements based on the RICE model to which our study in this paper also contributes.[1]

Despite their success, there are also several conceptual limitations with these models. First, they are typically not based on the dynamic general equilibrium paradigm with decentralized markets and optimizing private agents (see Hassler et al. (2016) for further discussion of this point). Instead, solutions are derived from aggregate planning problems typically parameterized in a given path of policy variables such as emissions or abatement. As a consequence, it is not possible to study the incentives set by climate policies at the level of private agents (consumers, firms) and to characterize these policies explicitly in terms of emissions taxes. Moreover, it is also not possible to obtain an analytical characterization of optimal climate policies as in GHKT and analyze how they are shaped by deep model parameters.

In addition, deriving solutions in the RICE model requires strong additional restrictions such as no trade between regions (see Nordhaus & Yang (1996, p.747)). More importantly, these solutions are typically derived based on the concept of 'time-dependent Negishi weights' for which no theoretical foundation exists and the equivalence between equilibrium and Pareto-optimal allocations of the original approach in Negishi (1960) no longer holds. In fact, Dennig & Emmerling (2017) show that such weights distort regional intertemporal preferences and affect the implied discount and savings rates which may severely bias the quantitative results.

The dynamic general equilibrium framework employed in this paper permits to represent climate policies explicitly in terms of emissions taxes and to study their effects directly at the level of individual agents. In addition, we can characterize the optimal climate tax in closed form along with the range of Pareto-improving transfers between regions. Relative to the standard DICE-model, we also provide a much more detailed

---

[1]Examples are Carraro et al. (2006) who study transfer payments which make climate agreements self-enforcing, Eyckmans & Tulkens (2003) who consider transfers in climate agreements based on marginal damages, or Germain et al. (2003) who study transfers in a dynamic game under which regions are incentivized to cooperate.

description of the energy production stage and include important additional sources of regional heterogeneity in the analysis. Finally, like the RICE-model our framework also allows for an arbitrary number of regions but requires neither the strong restrictions on trade between regions nor is it based on the concept of time-dependent Negishi weights.

Simulating a model with multiple heterogeneous regions and different production sectors is computationally challenging. We develop a numerical algorithm based on the 'forward shooting'-technique (see Atolia & Buffie (2009), Judd (1992), or Trimborn et al. (2008)). A major advantage of this approach is that we can directly use the model's equilibrium conditions and do not have to use linearization or perturbation methods. This offers a fast, reliable, and transparent way to compute the equilibrium solution for a large set of climate policies in the presence of an arbitrary number of regions, different energy sectors, and various types of exhaustible resources. In fact, our algorithm could easily handle many more than the six regions assumed in our simulation study. It therefore offers a methodological contribution beyond its application in this paper.

The paper is organized as follows. Section 1 introduces the model. Section 2 describes our calibration strategy for the model's parameters. Section 3 presents and discusses the quantitative results for our baseline scenario. Section 4 performs a series of robustness checks and explores alternative model specifications. Section 5 discusses the scope and possible extensions of our results. Section 6 concludes, Appendices A and B provide detailed descriptions of our computational method to compute the dynamic equilibrium solution under alternative climate policies and the calibration of parameters.

1 The Model

This section introduces the main building blocks of our model and derives the decentralized equilibrium solution for a given climate policy.[2]

1.1 Production sectors

The economy evolves in discrete time $t \in \{0, 1, 2, \ldots\}$ and is divided into $L \geq 2$ different regions $\ell \in \mathbb{L} := \{1, \ldots, L\}$. The production process in each region $\ell \in \mathbb{L}$ consists of three stages. The *final stage* produces the consumption good using labor, capital, and energy as inputs. Energy goods are produced at the *energy stage* based on alternative clean and dirty technologies using capital, labor, and fossil fuels. The *resource stage* extracts and supplies fossil fuels.

Final stage
The final sector $i = 0$ in region $\ell \in \mathbb{L}$ produces output Y_t^ℓ in period t using capital $K_{0,t}^\ell$,

---

[2]See Hillebrand & Hillebrand (2019) for additional details on the model and formal proofs for the results presented in this section.

labor $N_{0,t}^\ell$, and a composite energy good E_t^ℓ as inputs. The production technology is

$$Y_t^\ell = (1 - D_t^\ell)(K_{0,t}^\ell)^{\alpha_0}(N_{0,t}^\ell)^{1-\alpha_0-\nu_0}(E_t^\ell)^{\nu_0} \tag{1}$$

where $D_t^\ell \in [0,1[$ is an index of climate damage which is further specified below. Energy E_t^ℓ is the composite of three energy goods which are aggregated as

$$E_t^\ell = \left[\kappa_1(E_{1,t}^\ell)^\varrho + \kappa_2(E_{2,t}^\ell)^\varrho + \kappa_3(E_{3,t}^\ell)^\varrho\right]^{\frac{1}{\varrho}} \quad \text{where} \quad \sum_{i=1}^{3} \kappa_i = 1. \tag{2}$$

Parameters $\kappa_i > 0$ in (2) define the relative productivity of energy good i while $\varrho < 1$ determines the elasticity of substitution $1/(1-\varrho)$ between different energy goods.

Given climate damage D_t^ℓ and prices r_t for capital, w_t^ℓ for labor, and $p_{i,t}^\ell$ for energy good i in period t, the final sector chooses factor inputs to maximize profits. The profit maximizing solution solves the standard first order conditions

$$\frac{\alpha_0 Y_t^\ell}{K_{0,t}^\ell} = r_t, \quad \frac{(1-\alpha_0-\nu_0)Y_t^\ell}{N_{0,t}^\ell} = w_t^\ell, \quad \text{and} \quad \frac{\nu_0 Y_t^\ell}{E_{i,t}^\ell}\kappa_i\left(\frac{E_{i,t}^\ell}{E_t^\ell}\right)^\varrho = p_{i,t}^\ell \quad \text{for } i = 1,2,3. \tag{3}$$

Energy stage

Each region $\ell \in \mathbb{L}$ has three energy sectors $i = 1,2,3$ which produce differentiated energy goods $E_{i,t}^\ell$ using capital $K_{i,t}^\ell$ and labor $N_{i,t}^\ell$ in period t. The first two sectors $i = 1,2$ use, in addition, an exhaustible resource input $X_{i,t}^\ell$. Their production technologies are

$$E_{i,t}^\ell = Q_i^\ell\left(K_{i,t}^\ell\right)^{\alpha_i}\left(N_{i,t}^\ell\right)^{1-\alpha_i-\nu_i}\left(X_{i,t}^\ell\right)^{\nu_i}, \quad i = 1,2. \tag{4}$$

Here, $Q_i^\ell > 0$ is a constant productivity parameter. Usage of exhaustible resources $X_{i,t}^\ell$ generates proportional emissions of carbon dioxide (CO_2) given by

$$Z_{i,t}^\ell = \zeta_i X_{i,t}^\ell, \quad i = 1,2. \tag{5}$$

Parameter ζ_i is the physically determined carbon-content of exhaustible resource i. Energy sectors thus represent the production stage at which emissions occur. We assume that region ℓ imposes a tax $\tau_t^\ell \geq 0$ (which may be zero) on emissions in period t.

Let $v_{i,t}$ denote the world price of exhaustible resource i in period t. Given the tax and factor prices, both sectors $i = 1,2$ choose factor inputs to maximize profits. The first order conditions necessary and sufficient for an optimal solution take the form

$$\frac{\alpha_i p_{i,t}^\ell E_{i,t}^\ell}{K_{i,t}^\ell} = r_t, \quad \frac{(1-\alpha_i-\nu_i)p_{i,t}^\ell E_{i,t}^\ell}{N_{i,t}^\ell} = w_t^\ell, \quad \text{and} \quad \frac{\nu_i p_{i,t}^\ell E_{i,t}^\ell}{X_{i,t}^\ell} = v_{i,t} + \zeta_i \tau_t^\ell \quad \text{for } i = 1,2. \tag{6}$$

The third energy sector $i = 3$ operates a clean technology based on renewable sources like wind, water, and solar energy which do not enter as production inputs and do not cause emissions. The production technology in this sector is

$$E_{3,t}^\ell = Q_3^\ell\left(K_{3,t}^\ell\right)^{\alpha_3}\left(N_{3,t}^\ell\right)^{1-\alpha_3} \tag{7}$$

where $Q_3^\ell > 0$ is again a constant productivity parameter. The optimality conditions necessary and sufficient for profit maximization read

$$\frac{\alpha_3 p_{3,t}^\ell E_{3,t}^\ell}{K_{3,t}^\ell} = r_t \quad \text{and} \quad \frac{(1 - \alpha_3 - \nu_3) p_{3,t}^\ell E_{3,t}^\ell}{N_{3,t}^\ell} = w_t^\ell. \tag{8}$$

In the sequel, we define the set of production sectors $\mathbb{I}_0 := \{0, 1, 2, 3\}$ and the set of energy sectors $\mathbb{I} := \{1, 2, 3\}$. Linear homogeneity of the production technologies (1), (4), and (7) implies that profits are zero in each sector $i \in \mathbb{I}_0$.

Resource sectors

Exhaustible resources are identified by the same index $i = 1, 2$ as the energy sector which uses this resource in production. Denote by $R_{i,0}^\ell \geq 0$ the initial stock of resource i in region ℓ at time $t = 0$ and by $c_i > 0$ the constant extraction costs per unit of the resource. Profits in future periods $t \geq 0$ are discounted by the factor $q_t := \prod_{s=1}^t r_s^{-1}$ where $q_0 = 1$. Given the sequence of resource prices $(v_{i,t})_{t \geq 0}$, resource sector i in region ℓ chooses a non-negative extraction sequence $(X_{i,t}^{\ell,s})_{t \geq 0}$ which maximizes the discounted profit stream $\Pi_i^\ell := \sum_{t=0}^\infty q_t (v_{i,t} - c_i) X_{i,t}^{\ell,s}$ subject to the feasibility constraint

$$\sum_{t=0}^\infty X_{i,t}^{\ell,s} \leq R_{i,0}^\ell. \tag{9}$$

Linearity of the extraction technology implies that an optimal extraction plan exists if and only if resource prices satisfy $v_{i,0} \geq c_i$ and the Hotelling rule

$$v_{i,t} = c_i + r_t(v_{i,t-1} - c_i) \quad \text{for all } t > 0. \tag{10}$$

Clearly, only if $v_{i,0} = c_i$ may it be optimal not to deplete the entire resource stock. In either case, (10) permits equilibrium profits of resource sectors to be written as

$$\Pi_i^\ell = (v_{i,0} - c_i) R_{i,0}^\ell \quad \text{for } i = 1, 2. \tag{11}$$

1.2 Climate model

Emissions of CO_2 are generated by using ('burning') exhaustible fossil fuels like coal, oil, and gas in the production of energy. Total emissions in period t follow from (5) as

$$Z_t := \sum_{\ell \in \mathbb{L}} \left(Z_{1,t}^\ell + Z_{2,t}^\ell \right) = \sum_{\ell \in \mathbb{L}} \left(\zeta_1 X_{1,t}^\ell + \zeta_2 X_{2,t}^\ell \right). \tag{12}$$

Our standard scenario uses the climate model from GHKT where the climate state in period t consists of permanent ($S_{1,t}$) and non-permanent ($S_{2,t}$) CO_2 in the atmosphere.[3] Given an emissions sequence $\{Z_t\}_{t \geq 0}$ determined by (12), the climate state evolves as

$$S_{1,t} = S_{1,t-1} + \phi_L Z_t \tag{13a}$$
$$S_{2,t} = (1 - \phi) S_{2,t-1} + (1 - \phi_L) \phi_0 Z_t. \tag{13b}$$

---

[3]We discuss alternative climate models in the robustness analysis in Section 4.3.

Specification (13) assumes that a share $0 \leq \phi_L < 1$ of emissions become permanent CO_2. Out of the remaining emissions, a share ϕ_0 becomes non-permanent CO_2 which decays at constant rate $0 < \phi < 1$ while the remaining share $1 - \phi_0$ leaves the atmosphere. Climate damages at time t are determined by total atmospheric CO_2 concentration $S_t := S_{1,t} + S_{2,t}$ relative to the pre-industrial level $\bar{S}$ according to the damage function

$$D_t^\ell = D^\ell(S_t) := 1 - e^{-\gamma^\ell(S_t - \bar{S})}. \tag{14}$$

Regional differences in climate damage are captured by different parameters γ^ℓ, $\ell \in \mathbb{L}$.

1.3 Consumption sector

The consumption sector in each region $\ell \in \mathbb{L}$ consists of a single representative household which supplies labor and capital to the production process and decides about consumption and capital formation taking factor prices as given. In addition, the consumer is entitled to receive all profits from domestic firms and transfers from the government. Since profits in the final and energy sectors are zero, lifetime profit income of consumers in region $\ell \in \mathbb{L}$ follows from (11) as

$$\Pi^\ell = \sum_{i=1}^{2} \Pi_i^\ell = \sum_{i=1}^{2} (v_{i,0} - c_i) R_{i,0}^\ell. \tag{15}$$

The household's preferences over non-negative consumption sequences $(C_t^\ell)_{t \geq 0}$ are represented by a standard time-additive utility function

$$U((C_t^\ell)_{t \geq 0}) = \sum_{t=0}^{\infty} \beta^t u(C_t^\ell) \quad \text{where } u(C) = \frac{C^{1-\sigma} - 1}{1 - \sigma}, \quad \sigma > 0, 0 < \beta < 1. \tag{16}$$

Let K_0^ℓ denote initial capital in $t = 0$ and $N_t^{\ell,s} > 0$ the labor supplied in period t which is exogenous in our model. As before, let $q_t = \prod_{s=1}^{t} r_s^{-1}$ denote the discount factor for period t. Defining lifetime labor income $W^\ell := \sum_{t=0}^{\infty} q_t w_t^\ell N_t^{\ell,s}$, transfer income T^ℓ as in (25), and profit income Π^ℓ as in (15), consumers choose a non-negative consumption sequence $(C_t^\ell)_{t \geq 0}$ which maximizes utility (16) subject to their lifetime budget constraint

$$\sum_{t=0}^{\infty} q_t C_t^\ell \leq r_0 K_0^\ell + W^\ell + \Pi^\ell + T^\ell. \tag{17}$$

As shown in Hillebrand & Hillebrand (2019), optimal consumption in region $\ell \in \mathbb{L}$ is given by a constant share of world consumption $\bar{C}_t := \sum_{\ell \in \mathbb{L}} C_t^\ell$ in each period $t \geq 0$, i.e.,

$$C_t^\ell = \mu^\ell \bar{C}_t \quad \text{where} \quad \mu^\ell := \frac{r_0 K_0^\ell + W^\ell + \Pi^\ell + T^\ell}{\sum_{k \in \mathbb{L}} \left(r_0 K_0^k + W^k + \Pi^k + T^k \right)}. \tag{18}$$

The evolution of aggregate consumption is determined by the Euler equation

$$\bar{C}_{t+1} = (\beta r_{t+1})^{\frac{1}{\sigma}} \bar{C}_t \tag{19}$$

and must satisfy the transversality condition

$$\lim_{T \to \infty} \beta^T \bar{C}_T^{-\sigma} \bar{K}_{T+1} = 0 \tag{20}$$

where $\bar{K}_t$ is the aggregate world capital stock in period t.

1.4 Market clearing

Labor supply is immobile across regions and supplied to the domestic labor market. The market clearing condition for the labor market in region ℓ and period t reads

$$\sum_{i \in \mathbb{I}_0} N_{i,t}^\ell \overset{!}{=} N_t^{\ell,s}. \tag{21}$$

By contrast, capital, exhaustible resources, and final output can freely be traded between regions. Letting $\bar{K}_t > 0$ denote the world capital stock in period t, market clearing on the global capital market requires

$$\sum_{\ell \in \mathbb{L}} \sum_{i \in \mathbb{I}_0} K_{i,t}^\ell \overset{!}{=} \bar{K}_t. \tag{22}$$

The market clearing condition for resources $i = 1, 2$ in period t is $\sum_{\ell \in \mathbb{L}} X_{i,t}^{\ell,s} \overset{!}{=} \sum_{\ell \in \mathbb{L}} X_{i,t}^\ell$. Combining this constraint with (9) yields the world resource constraint

$$\sum_{t=0}^{\infty} \sum_{\ell \in \mathbb{L}} X_{i,t}^\ell \leq R_{i,0} \qquad \text{for } i = 1, 2. \tag{23}$$

Here, $R_{i,0} := \sum_{\ell \in \mathbb{L}} R_{i,0}^\ell$ denotes the global initial stock of the resource. As the Hotelling rule (10) makes resource firms indifferent between the timing of extraction, the amount $X_{i,t}^{\ell,s}$ extracted in a particular region and period is, in general, indeterminate.

Finally, denoting world consumption by $\bar{C}_t$ as before, the world capital stock evolves as

$$\bar{K}_{t+1} = \sum_{\ell \in \mathbb{L}} Y_t^\ell - \bar{C}_t - \sum_{i=1}^{2} c_i \sum_{\ell \in \mathbb{L}} X_{i,t}^\ell \qquad \text{for all } t \geq 0. \tag{24}$$

Equation (24) can be interpreted as a market clearing condition for final output.

1.5 Climate policy

Climate policy specifies the tax sequence $(\tau_t^\ell)_{t \geq 0}$ for each region ℓ. In the remainder of this and the following sections focus on the cooperative case where all regions choose an identical tax policy and pool tax revenue which are distributed according to a time-invariant transfer scheme. A non-cooperative scenario is studied in Section 3.4.

8

Formally, we assume that all regions choose the same tax sequence $\tau = (\tau_t)_{t \geq 0}$ (which may be zero). Global tax revenue is then distributed as lump-sum transfers to consumers in each region. We assume that regions agree on a time-invariant transfer policy $\theta = (\theta^\ell)_{\ell \in \mathbb{L}}$ satisfying $\sum_{\ell \in \mathbb{L}} \theta^\ell = 1$ which determines the share θ^ℓ of tax revenue received by region ℓ. This transfer policy constitutes the second part of a climate policy. Total discounted transfers received by consumers in region ℓ can be expressed as

$$T^\ell = \theta^\ell \sum_{t=0}^{\infty} q_t \tau_t \sum_{\ell \in \mathbb{L}} \left(\zeta_1 X_{1,t}^\ell + \zeta_2 X_{2,t}^\ell \right). \tag{25}$$

Note that the case $\theta^\ell < 0$ is not excluded in this definition, in which case consumers in region ℓ are taxed to finance transfers received by other countries. Thus, the previous specification also allows for international redistribution via lump-sum taxation. Our assumption of constant transfer shares is without loss of generality, since consumer behavior depends exclusively on lifetime transfers (25). Thus, one can show that any time-dependent distribution of transfers is equivalent to a transfer scheme with constant shares.

1.6   Equilibrium

Equilibrium with uniform taxation
The sequence $(\mathbf{N}_t^s)_{t \geq 0}$ of labor supplies $\mathbf{N}_t^s := (N_t^{\ell,s})_{\ell \in \mathbb{L}}$ is exogenously given in our model. Writing $\mathbf{Y}_t := (Y_t^\ell)_{\ell \in \mathbb{L}}$, $\mathbf{E}_t := (E_{i,t}^\ell)_{(\ell,i) \in \mathbb{L} \times \mathbb{I}}$, $\mathbf{K}_t := (K_{i,t}^\ell)_{(\ell,i) \in \mathbb{L} \times \mathbb{I}_0}$, $\mathbf{N}_t := (N_{i,t}^\ell)_{(\ell,i) \in \mathbb{L} \times \mathbb{I}_0}$, $\mathbf{X}_t := (X_{1,t}^\ell, X_{2,t}^\ell)_{\ell \in \mathbb{L}}$, $\mathbf{S}_t := (S_{1,t}, S_{2,t})$, $\mathbf{w}_t := (w_t^\ell)_{\ell \in \mathbb{L}}$, $\mathbf{p}_t := (p_{i,t}^\ell)_{(\ell,i) \in \mathbb{L} \times \mathbb{I}}$, and $\mathbf{v}_t := (v_{1,t}, v_{2,t})$ an aggregate equilibrium is a non-negative sequence $\xi = (\xi_t)_{t \geq 0}$ defined for each $t \geq 0$ as

$$\xi_t = (\mathbf{Y}_t, \mathbf{E}_t, \mathbf{K}_t, \mathbf{N}_t, \mathbf{X}_t, \mathbf{w}_t, r_t, \mathbf{p}_t, \mathbf{v}_t, \tau_t, \mathbf{S}_t, \bar{C}_t, \bar{K}_{t+1}) \tag{26}$$

which is consistent with the production technologies and optimality conditions (1)–(8) of producers, the Hotelling rule (10), the market clearing conditions (21), (22), and (24) for labor, capital, and output, the global resource constraint (23), and climate conditions (12)–(14) as well as the Euler equation (19) and transversality condition (20). The term 'aggregate' is used because ξ_t only involves aggregate consumption $\bar{C}_t$ but not its distribution across regions.

Previous definition of equilibrium requires to specify the tax policy $(\tau_t)_{t \geq 0}$ uniformly chosen by all regions. Two scenarios are of particular interest.

First, the *laissez-faire equilibrium* $\xi^{\text{LF}} = (\xi_t^{\text{LF}})_{t \geq 0}$ in which $\tau_t \equiv 0$. This represents the case where there is no attempt to correct market outcomes by imposing a climate tax. Due to the presence of a climate externality, this solution fails to be Pareto-optimal.

Second, the *efficient equilibrium* $\xi^{\text{eff}} = (\xi_t^{\text{eff}})_{t \geq 0}$ which maximizes utility of a fictitious world representative consumer to fully correct the inefficiency of the laissez-faire solution. Applying the results from Hillebrand & Hillebrand (2019), taxes along the efficient

equilibrium are determined by the Pigouvian solution

$$\tau_t = \sum_{n=0}^{\infty} \beta^n \left(\frac{\bar{C}_{t+n}}{\bar{C}_t}\right)^{-\sigma} \left(\phi_L + (1-\phi_L)\phi_0(1-\phi)^n\right) \sum_{\ell \in \mathbb{L}} \gamma^\ell Y_{t+n}^\ell. \tag{27}$$

The climate tax (27) is called the *efficient tax policy* and denoted by $\tau^{\text{eff}} = (\tau_t^{\text{eff}})_{t\geq 0}$. If the efficient allocation follows a balanced growth path on which output and consumption grow at constant and identical rate $g \geq 0$, (27) takes the simpler form

$$\tau_t^{\text{eff}} = \bar{\tau}^{\text{eff}} \sum_{\ell \in \mathbb{L}} \gamma^\ell Y_t^\ell, \quad \bar{\tau}^{\text{eff}} := \frac{\phi_L}{1 - \beta(1+g)^{1-\sigma}} + \phi_0 \frac{1-\phi_L}{1 - \beta(1+g)^{1-\sigma}(1-\phi)}. \tag{28}$$

Thus, on a balanced growth path, the optimal tax is a constant share $\bar{\tau}^{\text{eff}}$ of world output weighted by the damage parameters γ^ℓ. In our simulations, we determine optimal taxes based on (28) and show that it provides an excellent approximation to (27) even if the equilibrium is not exactly on a balanced path. We would also like to emphasize that the Cobb-Douglas form of the production technologies (1), (4), and (7) is not required to obtain the theoretical result (28). However, we make heavy use of the Cobb-Douglas forms in our computation algorithm described in Section A.

As the aggregate equilibrium solution (26) does not specify disaggregated consumption in each region, it is independent of the transfer policy $\theta = (\theta^\ell)_{\ell \in \mathbb{L}}$. Once such a transfer policy is specified, the consumption vector $C_t = (C_t^\ell)_{\ell \in \mathbb{L}}$ and the supporting transfers $(T^\ell)_{\ell \in \mathbb{L}}$ can be determined by (18) and (25). The main advantage of determining an aggregate allocation first is that the equilibrium equations give rise to a forward-recursive structure which greatly simplifies the computation of equilibrium solutions.

Equilibrium with regional taxation
The efficient equilibrium scenario assumes that all regions agree on a uniform carbon tax (27) which fully internalizes all current and future damages from emissions. An alternative scenario is the case where regions do not cooperate and instead choose taxes which are regionally optimal taking as given the decisions of other regions. In this case, we assume that the tax chosen by region ℓ in period t takes the form

$$\tau_t^\ell = \sum_{n=0}^{\infty} \beta^n \left(\frac{\bar{C}_{t+n}}{\bar{C}_t}\right)^{-\sigma} \left(\phi_L + (1-\phi_L)\phi_0(1-\phi)^n\right) \gamma^\ell Y_{t+n}^\ell. \tag{29}$$

Intuitively, the tax (30) only internalizes the domestic damages in region ℓ resulting from emissions at time t. Hillebrand & Hillebrand (2021) show that the solution (29) implements the open-loop Nash equilibrium in which each region maximizes domestic welfare (16) taking international prices and policies of other regions as given. Similar to (28), if the equilibrium allocation follows a balanced growth path where output and consumption grow at constant and identical rate $g \geq 0$, (29) takes the simpler form

$$\tau_t^\ell = \bar{\tau}^{\text{eff}} \gamma^\ell Y_t^\ell \tag{30}$$

with parameter $\bar{\tau}^{\text{eff}}$ defined as in (28).

1.7 Solving the Model

We develop a computational algorithm permitting to compute the aggregate equilibrium sequence $(\xi_t)_{t\geq 0}$ defined in (26) under alternative specifications of the climate tax policy $(\tau_t)_{t\geq 0}$. The details of this procedure can be found in Section A in the Appendix. We confine attention to policies where the tax is determined endogenously as

$$\tau_t = \bar{\tau} \sum_{\ell \in \mathbb{L}} \gamma^\ell Y_t^\ell, \quad \text{for all } t \geq 0. \tag{31}$$

Specification (31) induces the laissez-faire equilibrium by setting $\bar{\tau} = 0$ and the (approximated) efficient solution for $\bar{\tau} = \bar{\tau}^{\text{eff}}$ defined as in (28). It is also straightforward to modify our algorithm of Section A to solve for the non-cooperative equilibrium in which regional taxes are chosen based on (30). We explore this case as an additional scenario in our simulation study and present quantitative results in Section 3.4.

2 Model Calibration

This section develops the basic parametrization of our simulation model based on empirical observations and predictions. Our notational convention will be to add a 'bar' superscript to a parameter once a value has been assigned to it. This allows us to distinguish free parameters from those which have already been fixed by observation.

2.1 Regional structure and calibration targets

Regions and time structure
The world is divided into $L = 6$ regions which are listed in the following Table 1. Details on the composition of regions can be found in Section B.1 in Appendix B.

Table 1: Regions in the simulation model

Region	Label	Index ℓ	Region	Label	Index ℓ
United States	USA	1	China	CHN	4
OECD Europe	OEU	2	Developing Countries	DEC	5
Other High Income	OHI	3	Low Income Countries	LIC	6

One time period t in our model represents ten years which is a standard choice in the literature. The initial model period $t = 0$ represents the years 2006-2015 and is referred to as the baseline period 2010. Subsequent periods representing years $2016 - 2025$, $2026 - 2035$, etc. are referred to by their midpoints $2020, 2030$, etc. Flow variables such as production output or emissions are generally aggregated over the entire period while stocks such as capital or atmospheric carbon usually refer to the beginning of the period.

Energy sources and sectors

The exhaustible resources used in sector $i = 1$ represent oil and natural gas which are aggregated to a composite exhaustible resource. Energy goods and services produced in this sector comprise fuel-based transportation as well as electricity and heat generated from oil and gas. Sector $i = 2$ subsumes all energy goods and services based on coal which mainly consist of electricity and heat. The clean sector $i = 3$ subsumes all energy goods which do not cause emissions. This includes electricity based on renewable sources such as wind, water, or solar but also nuclear-based electricity and heat.[4]

Climate policies

Our results predict the evolution of the model economy under two political scenarios already mentioned before. The first scenario is the laissez faire case where emissions are not taxed and the climate problem is fully ignored. The second scenario assumes that all regions introduce the optimal emissions tax in the first period $t = 2020$. Thus, there is no taxation in the baseline period $t = 2010$ in both scenarios. We choose these two scenarios because they represent a best-case and worst-case outcome. In this sense, our results define the range of possible outcomes under alternative climate policies.

Main calibration targets

Table 2 lists a number of regional characteristics for the years 2006-2015 along with population forecasts for future periods that we match in our simulation study. Details on how we constructed the data can be found in Section B.2 in Appendix B.

Table 2: Calibration targets for baseline period 2006-2015 and population forecasts

Variable	Description	USA	OEU	OHI	CHN	DEC	LIC	World
$\bar{Y}_0^\ell$	GDP [Trn. U.S.$]	156.7	188.5	144.8	134.5	162.6	147.8	934.9
$\bar{X}_{1,0}^\ell$	Oil consumption [Gt]	13.9	10.3	12.7	5.3	15.5	7.4	68.0
$\bar{X}_{2,0}^\ell$	Coal consumption [Gt]	9.6	6.2	5.8	31.9	7.0	8.6	69.1
$\bar{n}_0^\ell$	Population in 2010 [mio.]	310	557	335	1341	1110	3289	6942
$\bar{n}_{19}^\ell$	Population in 2200 [mio.]	470	500	329	1201	1162	4825	8486

2.2 Climate and damage parameters

Climate parameters

Our model of the Carbon cycle (13) and damage function (14) is taken directly from GHKT. We also use their parameter values $\phi_L = 0.2$ implying that 20% of emissions become permanent, $\phi = 0.0228$ which determines the depreciation rate of non-permanent

---

[4]We do not include uranium as an explicit input to nuclear-based energy production in sector $i = 3$ although it is also an exhaustible resource. This seems justified, however, because the existing stocks of uranium are abundant relative to fossil reserves.

emissions and $\phi_0 = 0.393$ which is the share of non-permanent emissions escaping the atmosphere directly. We also set the pre-industrial CO_2-level to $\bar{S} = 581$ GtC.

Damage parameters

The damage parameters γ^ℓ in (14) are chosen consistent with empirically predicted climate damages for each region. Details are provided Section B.3 in Appendix B for details. Table 3 summarizes these values.

Table 3: Regional climate damage parameters

Parameter	USA	OEU	OHI	CHN	DEC	LIC
γ^ℓ	0.0000412	0.0000205	0.0000205	0.0000412	0.0000622	0.0000833

Initial climate state

The initial levels $S_{1,-1}$ for permanent and $S_{2,-1}$ for non-permanent CO_2 at the beginning of $t = 0$ are chosen to make the model consistent with the observed atmospheric CO_2 concentration $\bar{S}_{-1} = 807$ GtC in 2005 and $\bar{S}_0 = 851$ GtC in 2015 from ESRL (2016) as well as global emissions $\bar{Z}_0 = 92$ GtC from 2006-2015 from Boden et al. (2010). Using these targets in the climate model (13) yields the two conditions $\bar{S}_{-1} = S_{1,-1} + S_{2,-1} = 807$ and $\bar{S}_0 = S_{1,-1} + (1-\phi)S_{2,-1} + (\phi_L + (1-\phi_L)\phi_0)\bar{Z}_0 = 851$ which can be solved to determine the initial levels $S_{1,-1} = \bar{S}_{1,-1} = 658$ GtC of permanent and $S_{2,-1} = \bar{S}_{2,-1} = 149$ GtC of non-permanent carbon at the beginning of $t = 0$ corresponding to the year 2006.[5]

2.3   Predetermined production parameters

Capital elasticities

A major advantage of the Cobb-Douglas technologies (1), (4), and (7) is that we can calibrate the elasticities α_i based on the observed factor cost shares in production. For sector $i = 0$, we set $\alpha_0 = \bar{\alpha}_0 := 0.3$ which is a standard choice also used in GHKT.

For sector $i = 1$, we use input-output tables from the U.S Bureau of Economic Analysis (2007) which details the inter-sectoral linkages for 389 industries/commodities for the U.S. economy from which we isolate those sectors which provide energy goods and services based on oil and gas.[6] We then compute the aggregate labor costs of these sectors relative to their output which gives a labor cost share $1 - \alpha_1 - \nu_1 = 0.14$. Choosing

---

[5]Alternatively, we could have based our initial values on the empirical value $S_{-1} = 807$ GtC in 2005 and cumulative emissions $Z_{1750-2005} = 320$ GtC from 1750-2005 reported in ESRL (2016). This is the approach employed by GHKT. The choice $\phi_L = 0.2$ implies that one fifth of these emissions become permanent permitting to infer the initial climate state in 2005 from the pre-industrial level $\bar{S} = 581$ as $S_{1,-1} = \bar{S} + \phi_L Z_{1750-2005} = 581 + 64 = 645$ and $S_{2,-1} = S_{-1} - S_{1,-1} = 807 - 645 = 162$ GtC. The backward consistency of the employed climate model under the sequence of historical emissions is further explored in Section 4.3 and the results led us to favor our calibration strategy described above.

[6]This includes oil- and gas-based generation of electricity and heat as well as oil refineries and transportation services such as motor-vehicles, cargo aircrafts, railroad cargo etc.

$\alpha_1 = 0.272$ we match this share for the parameter ν_1 defined below in equation (A.18). As sectors $i = 2$ and 3 mainly produce electricity, we base our parameter choices on the nominal electricity generation costs from the OECD, IEA & NEA (2015) which provides direct estimates for the share of capital costs in production. For sector $i = 2$, we use the capital cost share under 10% depreciation which gives $\alpha_2 = 0.391$. The same source also reports a fuel cost share of 0.27 which is close to the value for $\nu_2 = 0.21$ chosen below. Since the renewable sector $i = 3$ comprises green technologies like wind or solar power but also nuclear power generation, we take the average capital cost share of emissions-free technologies weighted by their respective shares of output which gives $\alpha_3 = 0.82$. Our sensitivity analysis in Section 4 shows that none of these choices for capital elasticities is key for our results which are robust to alternative choices.

Elasticity of substitution between energy types
A key parameter in (2) is ρ which determines the elasticity of substitution $1/(1 - \rho)$ between different energy sources. Our standard value $\rho = \bar{\rho} = 0.5$ yields an elasticity of substitution equal to two. This choice is motivated by recent estimates from Papageorgiou et al. (2017) who argue that this elasticity 'significantly exceeds unity'. Acemoglu et al. (2012) consider an even higher value of three in their numerical applications. We consider an alternative much smaller choice in our sensitivity analysis in Section 4.

Initial resource stocks
For oil and gas, we aggregate empirically proven and estimated reserves for 2015 obtained from the Federal Institute for Geosciences and Natural Resources (2015). Using the values from Table 16 in Section B.4 yields a global resource stock $R_{1,1} = 394 + 924 = 1318$ Gt at the end of $t = 0$. Since we match the global extractions of 68 Gt of the resource in $t = 0$, we set $R_{1,0} = 1318 + 68 = 1386$ Gt for the initial stock in $t = 0$.
Unlike oil and gas, global stocks of coal are relatively abundant. Thus, we adopt the same arguments as GHKT and most other studies to assume that there is no scarcity rent on the resource. Formally, this corresponds to $R_{2,0} = \infty$ in our simulations which implies $\nu_{2,t} = c_2$ for all $t \geq 0$. However, all our results are essentially unchanged if we set $R_{2,0} = 1066.54 + 22415.94$ based on the total estimated reserves from Table 16.

Extraction costs and resource prices
We set $c_2 = 0.00043$ corresponding to extraction costs of 43 US$ per ton of coal. This choice is consistent with the value reported by the International Energy Agency (2010, p. 212) and also used by GHKT. Since $\nu_{2,t} \equiv c_2$, this is also the price of coal.
It is more difficult to measure extraction costs for oil and gas which differ considerably across regions and, in addition, often represent short term operating costs not including long-term capital costs. For this reason, our calibration strategy is to set the cost parameter c_1 such that the induced initial price $\nu_{1,0}$ of the resource is consistent with the empirically observed price obtained from Table 17 in Section B.5. This gives a target price $\nu_{1,0}$ of 403.3$ which we match by setting $c_1 = 0.00036969$ corresponding to extraction costs of 369.7$ per ton of the resource.

Carbon content
We determine the carbon content ζ_i of resources $i = 1, 2$ using observations for global primary energy consumption and emissions distinguished by fossil fuels from the IEA (2019). Dividing the observed cumulative emissions for 2006-2015 by the corresponding primary energy demand yields a carbon content of 648.2 KgC per ton of oil and 544.1 KgC per ton of coal. These correspond to $\zeta_1 = 0.6482$ and $\zeta_2 = 0.5441$ in our study.[7]

2.4 Calibrated production parameters

Energy elasticities and aggregation parameters
To infer the elasticities ν_i in (1) and (4) and the scaling factors κ_i in (2), we use U.S. data for physical and nominal final energy demand $\bar{E}_{i,0}^1$ and $\bar{E}_{i,0}^{1,\text{nom}} := \bar{p}_{i,0}^1 \bar{E}_{i,0}^1$ in $t = 0$ obtained from the U.S. Energy Information Administration (2019). The results are shown in Table 4. Details can be found in Section B.7 in the Appendix.

Table 4: Energy elasticities and aggregation

Parameter	Value	Parameter	Value	Parameter	Value
ν_0	0.0812	ν_1	0.5873	ν_2	0.2056
κ_1	0.53325	κ_2	0.29483	κ_3	0.17192

Productivity parameters
For each region $\ell \in \mathbb{L}$ we set total factor productivities Q_i^ℓ in (4) and (7) to match our targets for output $\bar{Y}_0^\ell$ and fossil fuel consumption $\bar{X}_{i,0}^\ell$, $i = 1, 2$ from Table 2 in the laissez-faire case. This yields the values in Table 5. Details can be found in Section B.8.

Table 5: Regional total factor productivity

Parameter	USA	OEU	OHI	CHN	DEC	LIC
Q_1^ℓ	1.38	0.56	0.85	0.11	0.36	0.06
Q_2^ℓ	10.19	3.56	4.07	6.96	1.66	0.73
Q_3^ℓ	111.49	360.61	116.10	12.70	24.22	41.99

2.5 Consumer sector

Preference parameters
Restricting consumer utility as in (16), we choose $\sigma = 1$ which gives a logarithmic utility

---

[7]Our carbon content of oil/gas is lower than the 844 KgC/t of oil used in GHKT. This is because our resource $i = 1$ also includes natural gas which has a lower carbon content than oil. In the case of coal, our values are based on an average of anthracite and lignite while GHKT only use the value of anthracite to obtain a carbon content of 716 KgC/t coal which is again higher than our value.

function. The annual discount rate is 1.5% which implies a discount factor $\beta = 0.985$[10]. These values are identical to the ones used by GHKT in their benchmark scenario. Alternative choices are discussed in the sensitivity analysis in Section 4.

Labor and productivity growth
Growth enters our model via labor-augmenting technical change which determines the evolution of labor supply $(N_t^{\ell,s})_{t\geq 0}$ in region $\ell \in \mathbb{L}$. We set $N_t^{\ell,s} = n_t^\ell a_t^\ell$ where n_t^ℓ represents the regional population size and a_t^ℓ labor productivity in period t. Our population sequence $(n_t^\ell)_{t\geq 0}$ matches the current and projected population size in $t = 2200$ listed in Table 2 and becomes constant thereafter. As for the productivity sequence $(a_t^\ell)_{t\geq 0}$, we assume a uniform long-run productivity growth rate of 1% p.a. Initial productivity levels are consistent with lower productivity in developing and poor countries. Growth rates are then chosen to ensure that aggregate GDP in in developing and poor countries catches up with aggregate GDP in rich countries well before 2100 in line with empirical projections. All details can be found in Section B.9 in the Appendix.

Initial capital and resource distribution
Our initial global capital stock is set to $\bar{K}_0 = 0.2375$. This value is chosen consistent with a stationary capital-to labor ratio to avoid a transitory effect due to capital adjustments in the initial periods. To compute the regional shares of consumption and transfers in Section 3.5 below we specify the initial distribution $(R_{1,0}^\ell)_{\ell \in \mathbb{L}}$ of exhaustible resource 1 based on Table 16. Since coal extraction generates zero profits, the distribution of the resource is irrelevant. Finally, we choose the initial distribution of capital $(K_0^\ell)_{\ell \in \mathbb{L}}$ based on empirically estimated financial wealth levels from the Credit Suisse Research Institute (2019). Details are provided in Section B.10.

3   Simulation Results

This section presents our simulation results for the standard parameter set developed in the previous section. Specifically, we compare the evolution of final output, fossil fuel consumption, and emissions at the regional level under both political scenarios as well as the evolution of global temperature and optimal taxes. We also quantify the range of Pareto-improving transfer payments between regions.[8]

3.1   Final output and growth

Regional gains and losses in GDP
A key measure to quantify the gains and losses from introducing the optimal tax policy is the change of final output (GDP) relative to the case with no taxation. Figure 1 depicts these changes in percentage terms for each region over the next 150 years.

---

[8]All simulation results can be downloaded at http://www.marten-hillebrand.de/research/
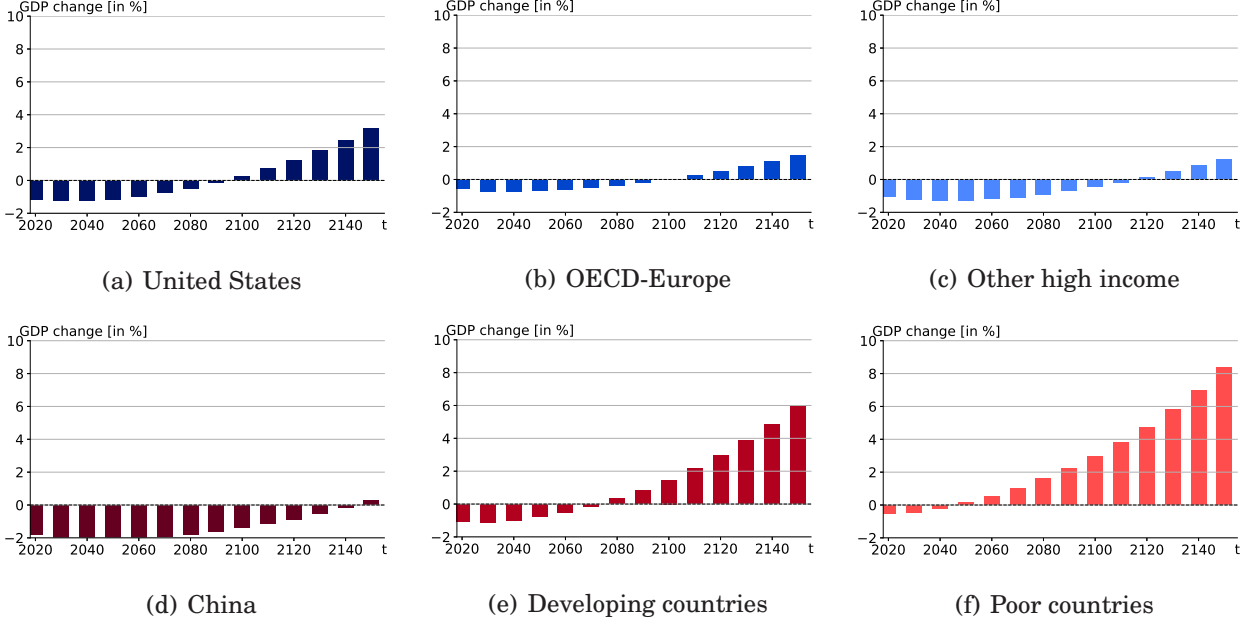
Figure 1: Gains and losses in GDP under optimal taxation relative to laissez-faire.

The figure confirms common intuition that climate policies come at initial costs but yield large gains in the long-run: GDP in each region is lower in the initial periods after the tax is introduced but higher in the long run. The size and duration of these 'adjustment costs' can be taken as a measure of how much each region benefits or suffers from the climate tax. In this sense, one observes that the costs and benefits are very different across regions: Low income countries (LIC) incur losses only in the first three decades until 2040 which are, in addition, confined to at most −0.5% of GDP. Thus, poor countries benefit most from the tax, followed by developing countries (DEC) where losses are at most −1.1% and last until $t = 2070$. This reflects our assumption that climate damages are most severe in these regions.

By contrast, China suffers most and incurs long-lasting losses in its GDP for over 120 years until 2140 which amount to −2% in the initial decades. The following sections will reveal that the optimal tax entails strong structural changes in Chinese energy production which is initially highly dependent of coal-based energy production.

Total adjustment costs

To further quantify the regional costs of joining the global climate agreement, let $(Y_t^{\ell,\mathrm{lf}})_{t \geq 0}$ and $(Y_t^{\ell,\mathrm{opt}})_{t \geq 0}$ denote the series' of GDP in region ℓ under the two policies and $(q_t^{\mathrm{lf}})_{t \geq 0}$ and $(q_t^{\mathrm{opt}})_{t \geq 0}$ be the associated discount factors defined in Section 1.3 which also depend on policies. We define the *cumulative adjustment costs* borne by region ℓ as

$$TC^\ell := \sum_{t=1}^{\infty} \max\left\{ q_t^{\mathrm{lf}} Y_t^{\ell,\mathrm{lf}} - q_t^{\mathrm{opt}} Y_t^{\ell,\mathrm{opt}}, 0 \right\}. \tag{32}$$

In words, TC^ℓ measures the total discounted GDP-losses under optimal taxation rel-

ative to the laissez-faire path. Table 6 quantifies these costs in absolute terms and relative to initial annual GDP in the respective region.

Table 6: Cumulative adjustment costs of optimal climate policy

	Region:	USA	OEU	OHI	CHN	DEC	LIC	World
TC^{ℓ}	[trillion U.S.$]	11.7	17.3	17.3	18.2	3.1	0.2	67.8
$TC^{\ell}/Y_0^{\ell,lf}\,p.a.$	[%]	74.7	92.0	119.7	135.0	18.8	1.4	72.5

At the global level, cumulative adjustment costs amount to almost 68 tr. U.S.$ or 72% of current annual world GDP. It is worthwhile to compare this number to a recent meta study by van Vuuren et al. 2020 who estimate the median of cumulative abatement costs (at 5% discount rate) for achieving the 2°-target to be 15 trillion U.S.$ and 30 trillion U.S.$ for the more ambitious 1.5°-target. The latter falls into a wide range of 10-100 trillion U.S.$ predicted by different models. Hence, our measure of total costs is in line with these numbers, but appears to be higher than many other estimates. The main insight, however, is that adjustment costs vary extremely at the regional level, ranging from just 1.4% of annual GDP in low income countries and as high as 135% in China. This confirms our earlier result from Figure 1 and suggest that the incentives to implement the optimal climate tax are also very different across regions, which appears to be the main obstacle for reaching a global climate agreement. Below we explore how transfers between regions can ensure that each region has an incentive to join the climate agreement.

3.2 Resource and energy stage

Consumption of fossil fuels
The calibration targets from Table 2 already show that initial energy production in all regions relies heavily on fossil fuels. In developed regions (USA, OEU, OHI) and also in developing countries (DEC), this dependence is more biased towards oil and gas which represents 59 to 69% of total fossil consumption in these regions. By contrast, energy production in China depends heavily on coal which makes up 86% of fossil fuels burnt in this region. One also observes that the two largest economies, the U.S. and China, consume more than 45% of global fossil fuels. This underscores the key role played by these two countries in any global climate agreement.

In this subsection we explore how regional dependence on fossil fuels evolves over the next 150 years depending on the climate policy adopted. Following table quantifies the immediate change of fossil fuel consumption in $t = 2020$ if the tax is introduced relative to the laissez-faire scenario.

Table 7: Change of fossil fuel consumption in $t = 2020$ under taxation

	Region:	USA	OEU	OHI	CHN	DEC	LIC	World
Oil consumption	[Gt]	-2.9	-2.3	-2.5	-0.7	-3.0	-1.8	-13.2
	[%]	-17.6	-21.2	-18.6	-13.6	-17.8	-20.3	-18.4
Coal consumption	[Gt]	-8.4	-4.8	-4.6	-23.9	-5.6	-7.6	-54.8
	[%]	-70.6	-71.9	-71.0	-69.1	-70.7	-71.6	-70.3

One notes that the reduction in oil consumption is rather moderate and varies roughly between 14% and 20% for all regions. By contrast, all regions must substantially reduce their coal consumption by about 70%, inducing a huge change in the energy mix. In absolute terms, the most drastic change is in China which must reduce its coal consumption by almost 24 Gt, which is equivalent to a reduction in emissions of 13 GtC or 48 $GtCO_2$.

Oil consumption
Figure 2 shows the evolution of regional oil consumption over the next 150 years. The solid black line is the sum of regional consumption which equals global extractions of the resource. In both scenarios, initial resource prices adjust to ensure that oil and gas

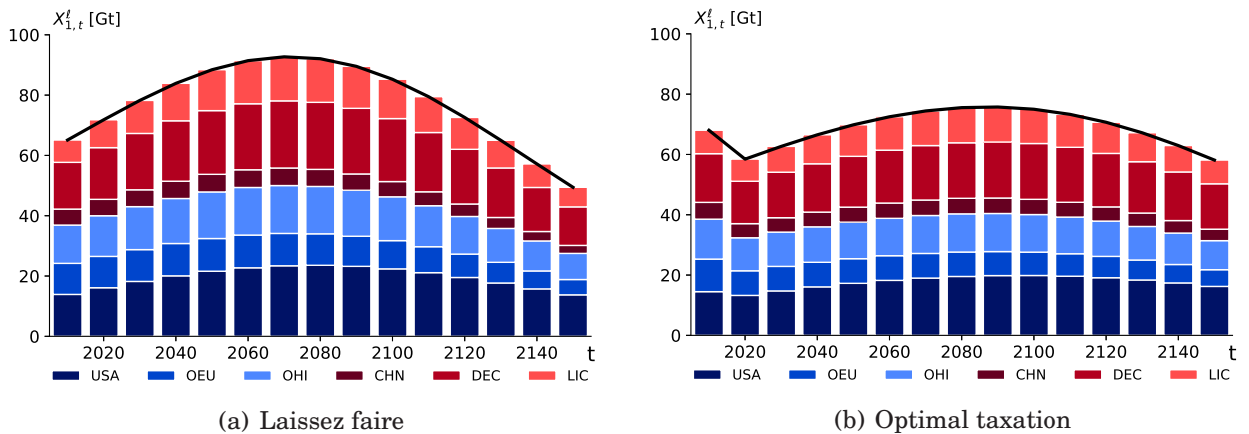(a) Laissez faire

(b) Optimal taxation

Figure 2: Regional consumption of oil and natural gas.

resources are fully depleted. In the absence of taxation, consumption increases during the initial periods to reach a maximum in 2070. This phenomenon, commonly referred to as 'peak oil', is line with empirical predictions. The same pattern is also present under optimal taxation where the peak occurs later in 2090, pushing oil extraction farther into the future. In this scenario, it is interesting to note that oil prices drop and extractions increase in $t = 0$ relative to laissez-faire. This 'green paradox' is due to the announcement effect of future taxation which discourages oil consumption in the future and has to be counteracted by a lower initial resource price to ensure that the resource is fully depleted. This is precisely the 'forgotten supply side' argument

advanced by Sinn (2012), see also Harstad (2012a). As a consequence, the carbon tax merely pushes oil and gas extractions back to the future by lowering it in the initial periods and increasing it in later periods with the total amount extracted unchanged.

Coal consumption
Figure 3 reports the paths of regional coal consumption and global extraction under the two political scenarios. Due to the absence of a scarcity rent, there is no adjustment in
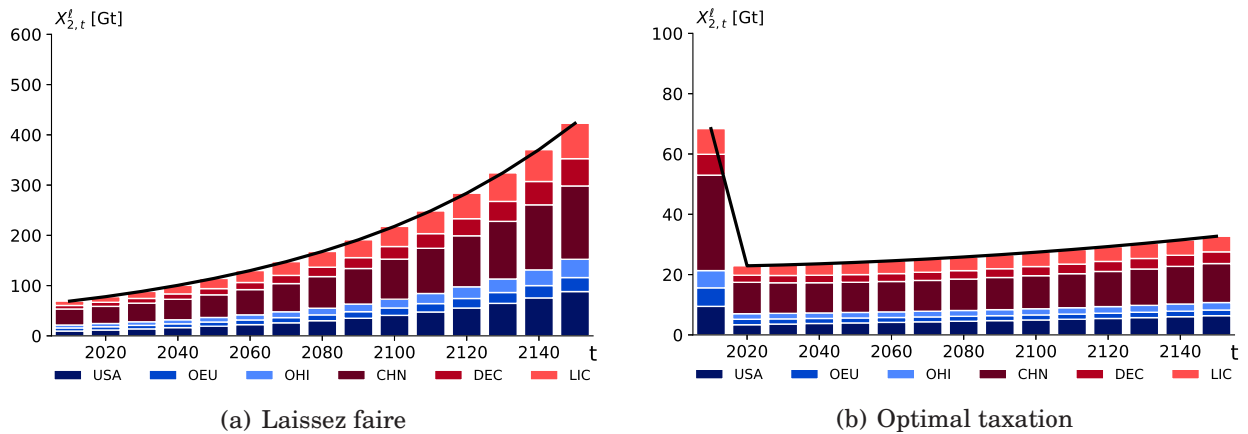

(a) Laissez faire

(b) Optimal taxation

Figure 3: Regional consumption of coal.

the market price of coal. As a consequence, both regional and global coal consumption respond strongly to climate policy. In the absence of taxation, consumption of the resource increases exponentially over the entire time window to reach a level of 420 Gt per decade in $t = 2150$. By contrast, introducing the optimal tax in $t = 1$ decreases coal consumption immediately, significantly, and permanently. It is this reduction in global coal consumption that is key for the success of climate policy. This also confirms the general insight that coal is the main driver of climate change emphasized in GHKT. At the regional level, the initial shares of coal consumption remain essentially unaltered over time, with China being the largest consumer of coal reserves in each of the following periods.

In summary, our results suggest that the decarbonization of regional energy production under the optimal policy is primarily driven by a reduction in coal consumption while oil extraction is merely pushed back to the future. In this process, China and the U.S. play a key role as these countries account for more than 60% of global coal consumption in the initial period. Thus, participation of these two regions is essential for the success of any climate agreement.

3.3 Climate stage

Emissions

The main criterion to evaluate the success of climate policy is whether it reduces emissions. Table 8 compares the observed regional CO_2-emissions reported by the IEA (2019) for the initial period with those generated by our model. The latter depends on whether or not the tax is introduced in $t = 2020$ due to the adjustment in initial resource prices.

Table 8: Emissions from fossil fuels $2006-2015$ in GtC

Region:	USA	OEU	OHI	CHN	DEC	LIC	World
Data[1]	14.2	10.1	11.2	21.5	12.9	10.2	80.1
Model (laissez-faire)	14.2	10.0	11.4	20.8	13.9	9.5	79.8
Model (optimal tax)	14.5	10.3	11.7	20.8	14.2	9.7	81.2

[1] Regional emissions from fossil fuels obtained from the IEA (2019)

The numbers confirm that our model generates initial emission levels fairly close to the empirical observations with only minor deviations in the laissez-faire case. We also see that introducing the optimal tax in $t = 2020$ increases emissions in $t = 2010$ due to the 'announcement effect' discussed above. In this counterfactual scenario, our model over-predicts the empirical values for most regions and also at the global level.

Figure 4 shows how these regional and global emissions evolve over time under both political scenarios. The result confirms that introducing the tax in $t = 1$ leads to a
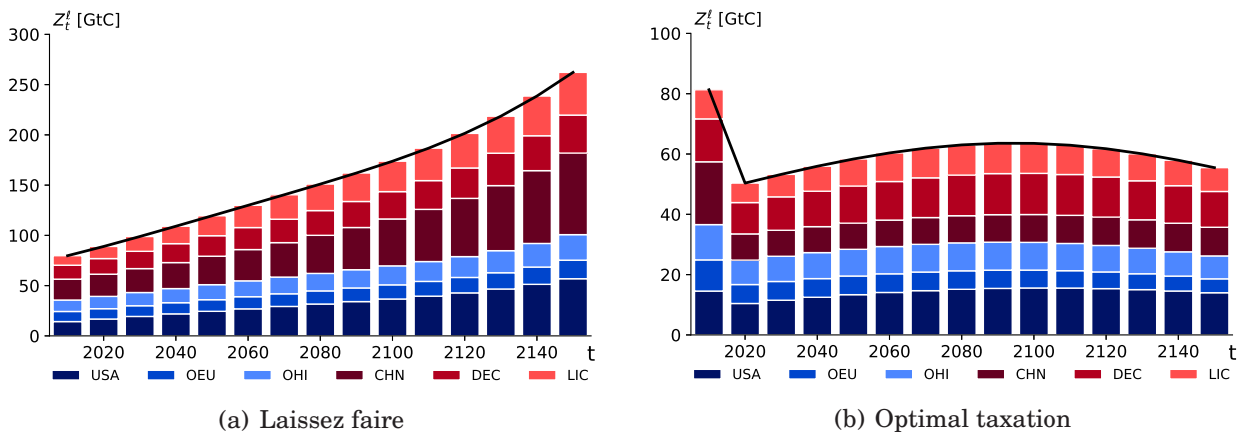

(a) Laissez faire

(b) Optimal taxation

Figure 4: Regional emissions from burning fossil fuel.

substantial and permanent reduction in emissions. At the global level, emissions in 2020 decline by about 43% relative to the laissez-faire equilibrium. In absolute terms, this corresponds to a reduction of -38.4 GtC or -140.7 Gt CO_2, which is a huge change.

At the regional level, there are again sizable differences depending on the initial degree of coal dependence. The most drastic reduction occurs in China where emissions decline by -13.5 GtC (-60.2%) relative to laissez-faire, followed by the U.S. where the decline is -6.4 GtC (-37.6%). These initial reductions are essentially preserved over the entire time window where emissions rise only slightly to reach a maximum after roughly 80 years in 2090. This is in stark contrast to the laissez-faire scenario where emissions continue to grow without bounds due to the exponential increase in coal consumption.

Climate tax and temperature

Figure 5(a) quantifies the price of carbon in $ per ton of CO_2 under optimal taxation. Since our computations employ the approximation formula (28), we also include the true values based on (27) to show that (28) provides an excellent approximation.
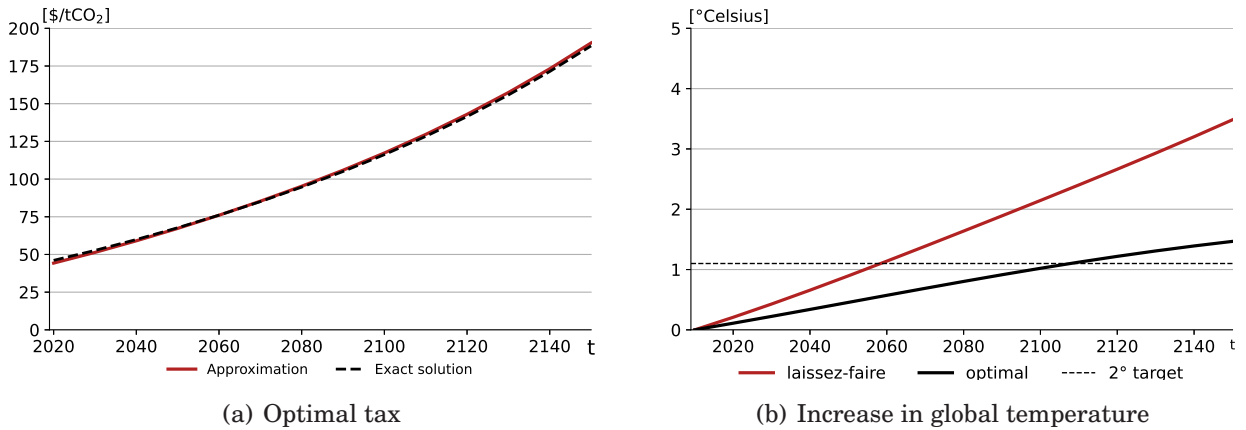

(a) Optimal tax
(b) Increase in global temperature

Figure 5: Social cost of carbon and increase in global temperature.

Quantitatively, the optimal tax amounts to 43.6 U.S. $ per ton of CO_2 in the initial period $t = 2020$. This value is in line with the 34$ reported in GHKT and also in Hillebrand & Hillebrand (2019) for the year 2010.[9] Our value is also higher than the optimal tax (corresponding to the social cost of carbon) obtained from the DICE model which amounts to 36.7 $/t CO_2 in $t = 2020$.[10] We also see that the optimal tax increases over time reflecting the growth trend of GDP in each region which must be accompanied a corresponding increase in the price of carbon emissions.

The main variable representing global warming and the success of climate policies is the change in global temperature. In our model we determine temperature by the so-called Arrhenius relation which is also used in GHKT and takes the form

$$TEMP_t = 3\log\left(S_t/\bar{S}\right)/\log 2. \tag{33}$$

[9]The increase is mainly due to GDP growth from 2010 to 2020 and also because we measure GDP in PPP-terms which increases measured GDP notably in less developed countries.

[10]The value is directly taken from the latest spreadsheet version of DICE available online at http://www.econ.yale.edu/~nordhaus/homepage/homepage/DICE2016R-090916ap-v2.xlsm.

Figure 5(b) shows the change in global temperature relative to the baseline period (right) for both political scenarios. An important benchmark is the 2°-target set by the 2015 Paris Agreement (cf. UNFCCC (2015)) which limits the increase in global temperature to less than two degrees until 2100 relative to the pre-industrial level. Data from NASA (2018) shows that global temperature in 2015 already exceeded the pre-industrial level by 0.9 °C. For this reason, the two-degree target corresponds to an additional increases of 1.1 °C relative to 2015. This critical level is represented by the dashed line in Figure 5(b). The main insight here is that under optimal taxation global temperature increases by 1.025 °C until 2100 which is therefore in line with the two-degree target. By contrast, the two-degree target is exceeded as early as 2060 under laissez-faire and increases exponentially thereafter. Quantitatively, these findings are in close conformity with the fifth assessment report by the IPCC (2015). This study asserts that the increase in global temperature can still be limited to 2 °C relative to pre-industrial levels if strict climate policies are adopted while the 'global climate budget' will be exhausted within the next 30 years if no actions are taken.

3.4   The non-cooperative solution

The climate policies studied so far represent two polar cases of perfect cooperation where regions agree to either ignore or to fully internalize the climate externality. In this section, we explore the non-cooperative case where all regions choose regionally optimal taxes (29) instead of the globally optimal tax (27). Intuitively, this leads to lower-than optimal taxation because regions just internalize the domestic damages from their emissions. Using the same parametrization as in the previous sections, Ta-

Table 9: Initial taxes in 2020 under cooperation and non-cooperation.

Region:	USA	OEU	OHI	CHN	DEC	LIC
Non-cooperative taxes in $/tCO$_2$	7.27	3.82	3.00	5.50	10.44	13.85
Fully-cooperative taxes in $/tCO$_2$	43.58	43.58	43.58	43.58	43.58	43.58

ble 9 quantifies the regionally optimal tax levels in the initial period $t = 1$ and compares it to the cooperative scenario with optimal taxation. It confirms that regionally optimal taxes are smaller by an order of magnitude than the optimal level. Regional deviations depend on the relative size of GDP and the extend of climate damages.

Figure 6 portrays the evolution of emissions taxes over time. Regionally optimal taxes mirror the growth path of the economy but remain much lower than the optimal level. For this reason, the non-cooperative equilibrium solution defines an intermediate case that falls into the range defined by the two policies studied in the previous sections. The same would hold for cases with partial cooperation where some regions form coalitions and jointly decide on taxes maximizing their collective welfare. In this sense, the

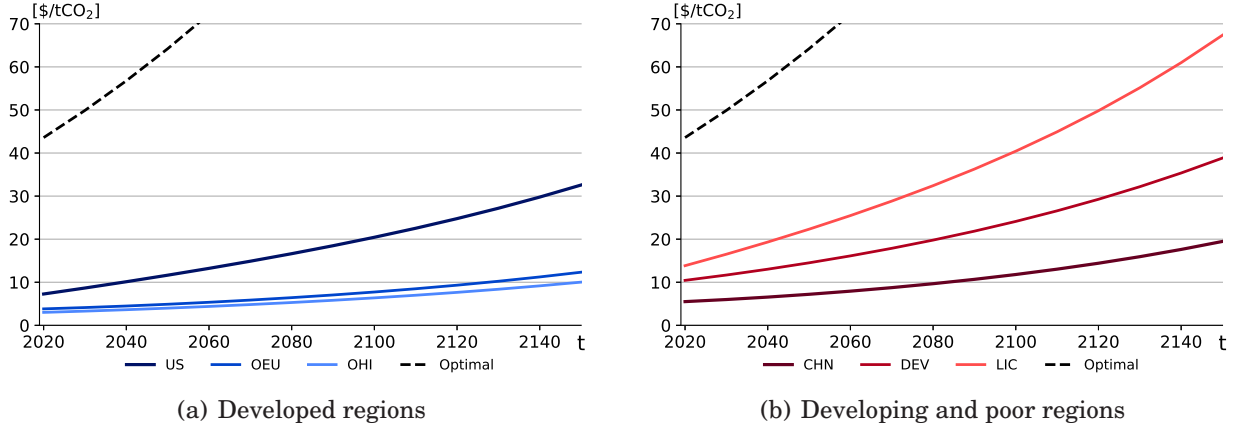(a) Developed regions   (b) Developing and poor regions

Figure 6: Taxation under non-cooperation.

quantitative results of our study define upper and lower bounds for the full class of all relevant climate policies. Moreover, due to the small amount of taxation under non-cooperation, our results would remain virtually unchanged if instead of the laissez-faire equilibrium the non-cooperative solution was used as a benchmark relative to which the gains and losses from optimal taxation are evaluated.

3.5 Pareto-improving transfer policies

Transfers and regional consumption shares
All of the previous results involve only the aggregate equilibrium (26) and, therefore, are independent of the transfer policy $\theta = (\theta^\ell)_{\ell \in \mathbb{L}}$ which determines how tax revenue is distributed across regions. As shown in Hillebrand & Hillebrand (2019), the choice of a transfer policy is equivalent to specifying a (target) consumption distribution $\mu = (\mu^\ell)_{\ell \in \mathbb{L}}$ which determines consumption in region ℓ as $C_t^\ell = \mu^\ell \bar{C}_t$, $t \geq 0$. Formally, the share of transfers θ^ℓ received by region ℓ and its consumption share μ^ℓ are related by

$$\theta^\ell = \frac{\mu^\ell \left[\sum_{k \in \mathbb{L}} \left(W^k + \Pi^k + r_0 K_0^k \right) + T \right] - W^\ell - \Pi^\ell - r_0 K_0^\ell}{T}, \quad T := \sum_{\ell \in \mathbb{L}} T^\ell \quad (34)$$

where the quantities entering (34) are defined as in Section 1 and computed numerically as explained in Section A.5. Note that θ^ℓ may be negative, in which case region ℓ imposes a lump sum tax on domestic consumers to finance transfers to other regions.

Optimal consumption and transfer shares
A particular transfer policy denoted by $\theta_{LF} = (\theta_{LF}^\ell)_{\ell \in \mathbb{L}}$ preserves the consumption distribution $\mu_{LF} = (\mu_{LF}^\ell)_{\ell \in \mathbb{L}}$ from the laissez-faire equilibrium under optimal taxation. This policy was shown in Hillebrand & Hillebrand (2019) to lead to a Pareto-improvement such that each region enjoys higher utility under optimal taxation than at the laissez-faire equilibrium. Quantitatively, we find that the welfare gains under this policy to

24

be a little more than 2% in consumption equivalents. This means that consumption at the laissez-faire equilibrium would have to be increased by 2% in every period for each region to enjoy the same utility as under optimal taxation.

Based on this result, we can compute the unique critical consumption share $\mu^\ell_{\min} < \mu^\ell_{LF}$ which region ℓ must at least receive in the equilibrium under optimal taxation to be better-off relative to laissez-faire. Further, we can use $\mu^\ell_{\min}$ in (34) to compute the minimal transfer share $\theta^\ell_{\min}$ which region ℓ must at least receive to prefer a climate agreement where each region implements the optimal tax policy over laissez-faire. If this number is negative, consumers in region ℓ would still benefit from the climate agreement if they paid an additional (small) lump-sum tax on their income. Table 10 reports these minimal consumption and transfer shares for our simulation study.

Table 10: Minimal Pareto-improving consumption and transfer shares.

Region:	USA	OEU	OHI	CHN	DEC	LIC	Sum
$\mu^\ell_{\min}$	0.1959	0.1801	0.1419	0.1276	0.1600	0.1726	0.9780
$\theta^\ell_{\min}$	-0.1492	-0.1019	0.0469	0.0351	-0.1803	-0.6451	-0.9945

The first row in Table 10 reveals that the U.S. must receive at least 19.59% of global consumption under optimal taxation to be better-off relative to Laissez-faire. The other entries have a similar interpretation. Note that consumption shares in our model are based on lifetime incomes and, therefore, reflect not only the current world income distribution (which would be much more biased towards developed countries) but also incorporate future growth prospects. The strict Pareto improvement over laissez-faire is reflected by the fact that the sum of minimal consumption shares is less than one.

The second row states that the U.S. will exactly attain its critical consumption share if it received no transfers but instead imposed a lump-sum tax on its consumers equal to 14.92% of global tax revenue. Thus, the benefit from the optimal tax is so large that U.S. consumers could still afford to subsidize other regions via lump-sum tax payments up to the critical amount. Qualitatively, the same holds for all other regions except for OHI-countries and China which need to receive at least 3.51% respectively 4.69% of global tax revenue in each period to be better-off under optimal taxation relative to the laissez-faire scenario. This result confirms our earlier insights that these regions suffer most in terms of initial GDP losses and need more than 100 years and even 140 years in the case of China to reap the benefits from the optimal tax.

The next Table 11 quantifies these minimal transfer payments in absolute terms in each year over the next five decades. One observes that China must receive annual transfers of initially 28.4 and later up to 56.9 billion U.S.$ to benefit from the global climate agreement. For OHI-countries, the transfers amount to initially 37.9 and later up to 75.9 billion U.S.$. By contrast, all other countries would even be willing to raise additional revenue from taxing their consumers to ensure that the global climate agreement

Table 11: Tax revenue and minimal Pareto-improving transfers p.a. [Bill. $]

Year	Tax revenue	Minimal annual transfers						Global funds
		USA	OEU	OHI	CHN	DEC	LIC	
2020	807.5	-120.5	-82.3	37.9	28.4	-145.6	-520.9	1610.5
2030	980.4	-146.3	-99.9	46.0	34.4	-176.8	-632.5	1955.4
2040	1174.9	-175.4	-119.7	55.1	41.3	-211.8	-757.9	2343.4
2050	1388.5	-207.2	-141.5	65.1	48.8	-250.3	-895.7	2769.4
2060	1618.8	-241.6	-165.0	75.9	56.9	-291.9	-1044.3	3228.6

is sustained. This willingness to pay for the success of the climate agreement is particularly striking for low-income countries: This region would be willing to contribute more than 500 billion U.S.$ p.a. in the initial years which increases to more than 1 trillion U.S.$ over the course of the next 40 years. Again, this confirms the earlier result from Figure 1 that poor countries benefit most from the optimal tax.

These results show that if each region received just the minimal transfer payments, annual global funds of 1.6 trillion U.S.$ from 2016-2025 and of 3.2 trillion from 2056-2065 would be available to be freely distributed across different regions without violating individual participation constraints. Clearly, the precise distribution would be determined by the bargaining process between regions that could be shaped by political power but also by common perceptions of fairness, severity of regional climate damages, etc. In this sense, our analysis provides only upper bounds for the size of transfer payments that all regions could agree on in a successful climate agreement.

It is interesting to note from Tables 10 and 11 that OHI countries claim a larger share of transfers than China despite GDP losses being smaller than in China (cf. Table 6). The reason is that OHI countries own higher stocks of oil (Table 16) which are devalued due to a lower resource price under optimal taxation. Thus, these countries are compensated not only for GDP losses but also for lower revenue from extracting fossil fuels.

4   Robustness

This section explores how alternative choices of pre-determined parameters affect our results. For each modification, we re-calibrated the parameter set following the same procedure as in the previous section. Below we also study the backward-consistency of the employed climate model under historical emissions and how an alternative specification with delayed climate damages affects the optimal climate tax in our model.

4.1 Production sector

Elasticity of energy substitution

Our standard choice $\rho = 0.5$ induces a relatively high elasticity of substitution between different energy goods. We therefore study a somewhat opposite extreme which sets $\rho = -1$ inducing an elasticity of substitution of $\frac{1}{2}$ such that the different energy goods are complements. A first consequence of this alternative choice is that the calibrated productivity parameters κ_i in (2) are now heavily biased towards oil. This can directly be verified from equation (A.16) which now produces ratios $\kappa_1/\kappa_2 = 32.82$ and $\kappa_1/\kappa_3 = 55.83$. Intuitively, the extremely high share of oil in the U.S. energy mix (both in monetary and in energy units) in the presence of imperfect substitution with other energy inputs can only be explained if the productivity parameter κ_1 is extremely high.

The most notable change in our simulation results is that coal consumption under laissez-faire now increases much slower than in the standard case. The intuition is that coal is no longer a good substitute for oil which declines over time due to its exhaustibility. This implies that the temperature increase under laissez-faire and the reduction in emissions due to taxation are also lower, although the tax is about the same as before. As a consequence, regions benefit less from the climate tax and, therefore, are also less willing to pay transfers to other regions. In fact, all regions except for OECD Europe and low income countries now demand compensation for introducing the optimal tax corresponding to a positive minimal transfer share in Table 10.

These results are further amplified if we replace (2) by the two-stage energy aggregator

$$E_t^\ell = \left[\kappa(E_{f,t}^\ell)^\rho + (1-\kappa)(E_{3,t}^\ell)^\rho\right]^{\frac{1}{\rho}} \text{ where } E_{f,t}^\ell = \left[\kappa_f(E_{1,t}^\ell)^{\rho_f} + (1-\kappa_f)(E_{2,t}^\ell)^{\rho_f}\right]^{\frac{1}{\rho_f}}. \quad (35)$$

This form allows us to disentangle the elasticity of substitution $1/(1-\rho_f)$ between energy types generated by different kinds of fossil fuels and the elasticity of substitution $1/(1-\rho)$ between clean and dirty energy.[11] Choosing $\rho = 0.5$ and $\rho_f = -1$ induces low substitutability between fossil-fuel based energies but high substitutability between fossil and clean energy. Coal consumption being tied to oil consumption now increases much slower under laissez-faire, leading to lower emissions and temperature and, therefore, smaller contributions from all regions due the low benefits from taxation. Conversely, for $\rho = -1$ and $\rho_f = 0.5$, substitutability between fossil energies is high but low between clean and dirty energy. This unleashes coal consumption under laissez-faire which substitutes for declining oil reserves and leads to massive increases in emissions and temperature. In such cases, a tax is highly effective and desired by all regions which provide large additional contributions to finance transfers to other regions. In this case, total funds available for transfers amount to more than 2.5 trillion U.S.\$ in t=2020 and almost 3.7 trillion in t=2060, which are both higher than the values from Table 11.

---

[11]Both our numerical algorithm and calibration strategy work exactly as before, with minor formal adjustments to the energy mix (A.2) which takes a slightly more complicated form. Setting $\rho = \rho_f$ and $\kappa_1 = \kappa\kappa_f$, $\kappa_2 = \kappa(1-\kappa_f)$, and $\kappa_3 = (1-\kappa)(1-\kappa_f)$ recovers the standard case.

Capital elasticities

We experimented with alternative choices for the pre-determined capital elasticities $\alpha_i, i = 1, 2, 3$ in the three energy sectors compatible with the values ν_i determined by (A.17). The main effect of more capital-intensive technologies at the energy state was a (small) increase in aggregate capital accumulation, as one would expect. Apart from that, none of our results on fossil fuel consumption, emissions, transfers, etc. was notably affected by such modifications. We therefore conclude that our findings do not hinge on the particular values employed in our study.

The case for Cobb-Douglas production

Our Cobb-Douglas specification for production in energy sectors (4) and (7) has several advantages. First, it is crucial for the algorithm laid out in detail in Section A.4 which crucially relies on the structure of first order conditions (A.4) obtained with Cobb-Douglas. Second, it allows us to discipline production parameters based on empirically observed cost shares in energy production.

An alternative specification of the technology (4) in exhaustible energy sectors $i = 1, 2$ would be a CES aggregator between fossil fuel inputs $X_{i,t}^{\ell}$ and a Cobb-Douglas aggregate of labor and capital. This form is assumed in Rezai & van der Ploeg (2015) who assume strong complementarity between energy and other factors in final production. At the level of energy production, complementarity between fossil fuels and other inputs seems also reasonable at the level of individual power plants. In our model, however, (4) is an aggregate technology representing an entire sector of plants which are typically quite heterogeneous with respect to their efficiency and capital intensity. Thus, during a sufficiently long time period (certainly for the ten years assumed in our model), the possibility of substituting new, highly efficient but more capital intensive plants for old, fuel-inefficient ones induces a much larger degree of substitutability between factors at the sectoral level. Hence, a Cobb-Douglas specification seems quite reasonable.

Initial resource stock oil/gas

The standard value for initial oil and gas reserves includes all proven and estimated reserves. A more conservative approach would be based only on confirmed reserves from Table 16 in which case $R_{1,0} = 394 + 68 = 462$ Gt in $t = 0$. For this scenario, oil extractions, emissions, and temperature are all lower than in the standard cases. Since oil reserves are smaller, they are substituted for by higher coal extractions which are maximally responsive to the climate tax due to the absence of a scarcity rent. For this reason, the climate tax has a higher social value and leads to higher minimal contribution rates for all regions than in the standard case, which increases total funds available for transfers.

4.2 Consumer sector

Discount factor

The decisive impact of the discount factor β on optimal climate taxes is well-known.

Since taxes determined by (28) in our model depend on β in exactly the same way as the optimal tax in GHKT, we refer to their discussion and notably their Figure 2 on page 70 which quantifies how changes in β affect the optimal climate tax.

Intertemporal elasticity of substitution

We studied two alternative cases with a higher value $\sigma = 2$ and a lower value $\sigma = 0.5$, respectively. This requires choosing a long-run growth parameter g in the tax approximation formula (28) which we set to $g = 0.1$ in both scenarios to obtain a good approximation to the true tax values determined by (27).

For the higher value $\sigma = 2$, a first major difference is a much lower Carbon tax which drops from previously 43.6\$ to a much lower value of 28.0\$ per ton of CO_2 in the initial period and is also lower by about 35-38% in all future periods. This results in a smaller reduction of coal consumption and emissions, slightly higher temperature, and a smaller gap between the two policy scenarios. Since the social benefits from introducing the optimal tax are now much smaller, all regions demand a positive share $\theta^\ell_{min} > 0$ of global transfers as compensation for the initial losses from the climate tax.

All these effects reverse if instead $\sigma = \frac{1}{2}$. The initial tax increases to a higher initial level of 62.5\$ and increases by about 41-43% in all future periods. This induces higher reductions in coal consumption and emissions, lower temperature, and higher social benefits from taxation. For this reason, all regions are willing to finance additional transfers via taxation corresponding to a negative minimal transfer share $\theta^\ell_{min} < 0$.

Labor productivity growth

Long-run productivity growth $\bar{g}_a$ in (A.25) is set to 1% per year in the standard case. Alternatively, we considered a lower value of 0.5% and a higher value of 1.5%. The lower value leads to smaller long-run emissions and temperature under laissez-faire which reduces the gains from the climate tax. Thus, minimal contribution rates from Table 10 are now lower and positive for all regions except low-income countries. These effects reverse if long-run productivity grows at 1.5% per year. In this case, the climate tax leads to large social gains by curbing temperature which otherwise would grow even more than in the standard case. Thus, all regions are willing to contribute large sums to enforce the climate agreement such that the global funds from Table 10 exceed 3 trillion U.S.\$ already in the initial period $t = 2020$. These results also confirm that economic growth induced by technological progress is a key driver of climate change.

4.3   Climate model

Delayed climate damages

A crucial feature of the climate model (13) and the associated damage function (14) is that emissions have an instantaneous impact on temperature and damage which is maximal in the period when they occur. An alternative climate model developed in Gerlagh & Liski (2018) stresses the delayed response of temperature and damages to

current emissions. To evaluate how this delay structure affects our optimal climate policy, we incorporated their three-layer climate model and damage function into our framework choosing the same parameter values as they do in their analysis. Hillebrand & Hillebrand (2019) show how the optimal tax (31) changes under this modification. The delayed response of climate damages to emissions reduces the optimal climate tax by about 38% such that the previous value of 43.6\$/t CO_2 in $t = 2020$ declines to a lower level of 27 \$/t CO_2. Thus, climate policy is much less aggressive and leads to lower social gains than in the standard case. This reduces the minimal transfer shares in Table 10 and most regions now demand compensation for introducing the climate tax.

Recent work by Dietz & Venmans (2019) finds that current economic models including Gerlagh & Liski (2018) tend to significantly overestimate the delay by which temperature responds to emissions. Thus, the instantaneous response assumed by the GHKT model and the delayed effect assumed by Gerlagh & Liski (2018) represent two extremes how climate damages respond to emissions. For this reason, the emissions taxes obtained in these two cases may be seen as defining the range of possible values. Quantitatively, these results are also in line with van den Bijgaart, Gerlagh & Liski (2016) who study the social cost of carbon for a large class of model specifications.

Backward consistency

A natural test for the specification of our climate model (13) and temperature equation (33) is whether it is consistent with empirical observations of atmospheric CO_2-concentration and temperature under historical emissions. Using data for emissions from 1750-2015 from Boden et al. (2010), we subjected our climate to this test and included two additional specifications in this experiment. First, the DICE model described in detail in Nordhaus & Boyer (2000).[12] Second, the HKOR-model from Hassler et al. (2020) which is also based on the GHKT climate model (13) but replaces equation (33) by the two-dimensional dynamic temperature model from DICE. Following table reports the outcome of our experiment.

The DICE model replicates the empirical figures fairly well, whereas the GHKT climate model under-predicts atmospheric CO_2 concentration by about 8% in both 2005 and 2015. This shortcoming is the reason why we did not calibrate our initial climate state in Section 2.2 based on historical emissions but instead on observations for 2005 and 2015. This under-prediction of carbon levels translates into atmospheric temperature lower than the empirical value in both the GHKT and the HKOR model.

By contrast, using the empirical CO_2 concentrations directly in our temperature equation (33) yields a predicted temperature increase of 1.4 in 2005 and 1.6 °C in 2015 which both exceed the empirical values. Thus, the equation (33) tends to over-predict

---

[12]We used the 2008 version of DICE which is available from the appendix (p.90-95) of the DICE 2013 manual in Nordhaus & Sztorc (2013) since is the last version of the model where one time period represents 10 years. The later 2013 and 2016 versions use 5-year time periods. We also disregard exogenous forcing and non-industrial emissions in our experiment which are part of the DICE equations.

Table 12: Backward consistency of different climate models

			Climate model		
Variable	Description	Data[1,2]	GHKT	HKOR	DICE
S_{2005}	Atmospheric CO_2 in 2005 [GtC]	807	739	739	798
S_{2015}	Atmospheric CO_2 in 2015 [GtC]	851	784	784	858
$Temp_{2005}$	Global temperature in 2005 [°C]	0.81	0.64	0.61	0.81
$Temp_{2015}$	Global temperature in 2015 [°C]	0.9	0.79	0.76	1.0

[1] Data on atmospheric carbon are from ESRL (2016)

[2] Temperature date are from NASA (2018)

temperature changes, a feature also noted in Nordhaus & Boyer (2000, p.66).

Reliability of temperature predictions

The previous results convey two important messages as to whether our predictions on global temperature in this paper are reliable. First, they show that the employed climate model tends to underestimate the accumulation of carbon in the atmosphere. Thus, even if our model matches the global emissions path, it might under-predict the resulting levels of atmospheric carbon and climate damages.[13] Second, as demonstrated above, formula (33) overstates the response of temperature to atmospheric levels of carbon. The result in Table 12 therefore suggests that these two effects cancel out to some extent providing a fairly accurate prediction of temperature changes over a relatively long stretch of time. For this reason, we are rather confident that our model generates reliable predictions of global temperature also for the future. Including alternative specifications of the climate-temperature dynamics similar to DICE without sacrificing analytical tractability of the overall model is one of our goals for future research.

5 Extensions and Discussion

In this final section we discuss some restrictions imposed by our study along with alternative specifications and possible extensions in future research.

5.1 World consumption distribution, convergence, and frictions

The assumption of a friction-less international capital market is crucial to obtain the separability result in Hillebrand & Hillebrand (2019) upon which the present paper builds. In fact, it is this assumption which permits to derive the optimal climate tax

---

[13]This is even more likely as our model considers only emissions from fossil fuels but abstracts from other sources such as cement production which make up a share of 3- 5% of historical emissions in Boden et al. (2010).

and Pareto-improving transfer shares in closed form. It is therefore a key ingredient to our analysis. A direct implication is that the world consumption distribution incorporates all future growth prospects of individual regions and, therefore, remains constant over time. Clearly, unconstrained international capital flows represent an idealized but important benchmark somewhat opposite to Hassler & Krusell (2012) and Hassler et al. (2020) who exclude such flows altogether. Introducing capital market imperfections such as borrowing constraints would lead to intermediate cases with arguably more realistic consumption distributions. This constitutes an important research objective.

In addition, it would be interesting to incorporate other frictions such as distortionary taxation studied in Barrage (2020) in our multi-region framework. Such extensions briefly discussed in Hillebrand & Hillebrand (2019) impose additional constraints on the optimal climate policy which may then be of a second-best nature. Even in such cases, however, the first-best scenario studied in this paper would constitute an important reference case relative to which any second-best climate policy could be evaluated.

5.2 Regional structure

Our choice of distinct regions aims to be large enough to incorporate the major players in actual climate agreements but small enough to present the quantitative implications for each region in a concise and comparable way. Since any multi-region study of climate change faces a trade-off between these two objectives, alternative specifications are conceivable as well. For example, India is a key developing country with large predicted economic and population growth and a major contributor to the climate problem due to its strong reliance on coal and could have been included as a separate region. The aggregation properties of our model established in Hillebrand & Hillebrand (2019) imply that such an extension would merely refine rather than substantially alter our quantitative results. From a computational perspective, an enlargement of the set of regions would be straightforward to include and the specification in this paper is not dictated by our numerical algorithm which could easily handle many more regions.

5.3 Climate damages and tipping points

Several recent studies employ a much more elaborate climate model permitting to incorporate a variety of additional features such as tipping points, parameter uncertainty or economic shocks, see for example Cai & Lontzek (2019). While the quantitative implications of such extensions are clearly important to understand, including them in our multi-region framework would necessitate major adjustments of both the theoretical model and the computational methods. In general, extensions of this kind will be confined to purely numerical results due to their complexity while the framework employed in this paper has the virtue of admitting theoretical insights as well.

6 Conclusions

How does a climate agreement to globally implement the optimal emissions tax affect different regions with heterogeneous economic and environmental characteristics? Our paper addresses this question in a quantitative study of a multi-region model calibrated to match key economic features of six major world regions. The climate policies under study are deliberately chosen to represent two extremes: A worst case scenario where the climate problem is completely ignored and a best case where all regions implement the optimal climate tax. In the first scenario, ever-increasing coal extractions lead to potentially devastating increases in global temperature and climate damages. Optimal taxation results in moderate temperature increases broadly in line with the two-degree target. However, this requires drastic cuts in fossil fuel and notably coal consumption which is reduced instantaneously by about -70% in each region corresponding to a global reduction of 5.5 Gt per year in $t = 2020$. Here, China and the U.S. play a key role as these two countries together account for more than 60% of the required reduction. These results were shown to be very robust under a broad set of alternative parameter specifications. Clearly, the figures are relative to a scenario where the climate problem is completely ignored. Since some countries have already implemented climate policies, this might overstate the actual reductions required.

We also constructed a measure of the cumulative adjustment costs associated with introducing the optimal tax to demonstrate that these costs are vastly different across regions. Designing a climate policy which incorporates the different characteristics and incentives of each region is therefore key for the success of a global agreement. To contribute to this discussion, we provided a complete characterization of the range and size of possible transfer payments between regions which respect each regions participation constraint. For the standard parametrization, we showed that most regions benefit so much from the optimal tax that they could afford to pay transfers to other regions. On an annual basis, these payments amount up to 1.6 trillion U.S.$ after introducing the global climate tax and increase to more than 3 trillion U.S.$ over the following four decades. Part of these funds would have to be used as direct transfers to China and a number of developed countries to ensure participation of these regions in the climate agreement. In addition, such funds could be used to support technological innovation and adaption notably in poorer regions most severely affected by climate damages.

These last results constitute a first step towards a more elaborate study of the bargaining process between regions as a cooperative or non-cooperative game as, e.g., in Harstad (2012b, 2016) or Hambel et al. (2021). First results derived in Hillebrand & Hillebrand (2021) suggest that our framework is amendable to such extensions as well. Modifications beyond the current framework are to include abatement costs and uncertainty, e.g., in climate damages and parameters, and endogenizing productivity growth due to directed technical change as, e.g., in Acemoglu et al. (2012).

A   Numerical Algorithm and Computational Details

A.1   Transforming the equilibrium conditions

We begin by performing a few transformations of the equilibrium conditions in period t. First, using (5), (12) and (13) in (14) and defining $\phi_Z := \phi_L + (1 - \phi_L)\phi_0$ permits to express climate damage in region ℓ as

$$D_t^\ell = 1 - \exp\left\{-\gamma^\ell\left(\phi_Z \sum_{k\in\mathbb{L}} \left(\zeta_1 X_{1,t}^k + \zeta_2 X_{2,t}^k\right) + S_{1,t-1} + (1-\phi)S_{2,t-1} - \bar{S}\right)\right\} \quad \text{for } \ell \in \mathbb{L}. \quad \text{(A.1)}$$

Second, to cast the firms' optimality conditions (3), (6), and (8) in a more accessible form, define for each $t \geq 0$ and $\ell \in \mathbb{L}$ the following auxiliary variable

$$\eta_{i,t}^\ell := \frac{p_{i,t}^\ell E_{i,t}^\ell}{\sum_{j\in\mathbb{I}} p_{j,t}^\ell E_{j,t}^\ell} \quad \text{for } i = 1, 2, 3. \quad \text{(A.2)}$$

Economically, $\eta_{i,t}^\ell$ represents the value of energy of type i relative to the total value of energy employed in production. In what follows, we will refer to the vector $\eta_t^\ell := (\eta_{i,t}^\ell)_{i\in\mathbb{I}}$ as the (nominal) *energy mix* in region $\ell \in \mathbb{L}$ at time t. Note that η_t^ℓ takes values in the positive unit simplex $\Delta_+^3 := \{(\eta_1, \eta_2, \eta_3) \in \mathbb{R}_+^3 | \sum_{i=1}^3 \eta_i = 1\}$. Equation (3) implies that $\sum_{j\in\mathbb{I}} p_{j,t}^\ell E_{j,t}^\ell = \nu_0 Y_t^\ell$ permitting to express the energy mix in region $\ell \in \mathbb{L}$ as

$$\eta_{i,t}^\ell = \kappa_i \left(E_{i,t}^\ell / E_t^\ell\right)^\rho \quad \text{for } i = 1, 2, 3. \quad \text{(A.3)}$$

Using (A.3), the Hotelling rule (10), and the form of emissions taxes (31) we obtain the first order conditions (3), (6), and (8) for all $\ell \in \mathbb{L}$ in the following form:

$$w_t^\ell = \frac{(1 - \alpha_0 - \nu_0)Y_t^\ell}{N_{0,t}^\ell} = \frac{\nu_0(1 - \alpha_i - \nu_i)Y_t^\ell}{N_{i,t}^\ell}\eta_{i,t}^\ell \quad \text{for } i = 1, 2, 3 \quad \text{(A.4a)}$$

$$r_t = \frac{\alpha_0 Y_t^\ell}{K_{0,t}^\ell} = \frac{\nu_0 \alpha_i Y_t^\ell}{K_{i,t}^\ell}\eta_{i,t}^\ell \quad \text{for } i = 1, 2, 3 \quad \text{(A.4b)}$$

$$c_i + r_t(v_{i,t-1} - c_i) + \zeta_i \bar{\tau} \sum_{h\in\mathbb{L}} \gamma^h Y_t^h = \frac{\nu_0 \nu_i Y_t^\ell}{X_{i,t}^\ell}\eta_{i,t}^\ell \quad \text{for } i = 1, 2 \quad \text{(A.4c)}$$

where we set $\nu_3 = 0$ in (A.4a) to allow for a more compact notation.

A.2   Recursive structure of equilibrium

Our numerical algorithm exploits the forward-recursive structure of the model to determine the vector ξ_t defined in (26) as a function of ξ_{t-1} and exogenous variables. To make

this idea precise, partition the equilibrium vector for each $t \geq 0$ as $\xi_t = (\xi_t^1, \xi_t^2)$ where

$$\xi_t^1 := (\mathbf{Y}_t, \mathbf{E}_t, \mathbf{K}_t, \mathbf{N}_t, \mathbf{X}_t, \mathbf{w}_t, r_t) \in \Xi^1 := \mathbb{R}_{++}^L \times \mathbb{R}_{++}^{3L} \times \mathbb{R}_{++}^{4L} \times \mathbb{R}_{++}^{4L} \times \mathbb{R}_{++}^{2L} \times \mathbb{R}_{++}^L \times \mathbb{R}_{++} \quad \text{(A.5a)}$$

$$\xi_t^2 := (\mathbf{p}_t, \mathbf{v}_t, \tau_t, \mathbf{S}_t, \bar{C}_t, \bar{K}_{t+1}) \in \Xi^2 := \mathbb{R}_{++}^{3L} \times \prod_{i=1}^2 [c_i, \infty[\times \mathbb{R}_+ \times \mathbb{R}_{++}^2 \times \mathbb{R}_{++} \times \mathbb{R}_{++}. \quad \text{(A.5b)}$$

We also collect the relevant pre-determined variables in period $t \geq 0$ in a vector

$$\theta_t := (\mathbf{N}_t^s, \mathbf{v}_{t-1}, \mathbf{S}_{t-1}, \bar{C}_{t-1}, \bar{K}_t) \in \Theta := \mathbb{R}_{++}^L \times \prod_{i=1}^2 [c_i, \infty[\times \mathbb{R}_+^2 \times \mathbb{R}_{++} \times \mathbb{R}_{++}. \quad \text{(A.6)}$$

Note that θ_t consist of the exogenous variables $\mathbf{N}_t^s$ and pre-determined endogenous variables from ξ_{t-1}^2.

Given $\theta_t \in \Theta$, the main step in our numerical algorithm below is to determine the $M := 15L + 1$-dimensional vector ξ_t^1 jointly with the $5L$-dimensional auxiliary variable $(E_t^\ell, D_t^\ell, \eta_t^\ell)_{\ell \in \mathbb{L}}$ by simultaneously solving the $L + 2L + L$ production equations (1), (4), and (7), the $L + 1$ market clearing conditions (21) and (22), the $4L + 4L + 2L$ optimality conditions (A.4) and the $L + L + 3L$ auxilliary equations (2), (A.1), and (A.3). These conditions constitute a system of $4L + L + 1 + 10L + 5L = M + 5L$ non-linear equations that can potentially be solved uniquely. Eliminating the auxiliary variables $(E_t^\ell, D_t^\ell, \eta_t^\ell)_{\ell \in \mathbb{L}}$ using (2), (A.1), and (A.3), we are left with M equations which determine the M-dimensional variable ξ_t^1. Define the function $\Phi : \Xi^1 \times \Theta \to \mathbb{R}^M$ such that ξ_t^1 solves these M conditions for given $\theta_t \in \Theta$ if and only if $\Phi(\xi_t^1, \theta_t) = 0$. We refer to this as the problem of *computing the equilibrium production allocation*. In Section A.4 we develop an algorithm which offers a fast and reliable way to solve this problem.

Given the solution ξ_t^1 and pre-determined variables θ_t, the components of ξ_t^2 can be determined directly by equations (3), (10), (31), (12) and (13), (19), and (24). These conditions define an explicit mapping $\Psi : \Xi^1 \times \Theta \to \Xi^2$ such that $\xi_t^2 = \Psi(\xi_t^1, \theta_t)$.

Determining ξ_t^1 and ξ_t^2 in this fashion based on predetermined variables collected in θ_t defines one iteration step of our model.

A.3 Numerical algorithm

Using the model's forward recursive structure identified previously, our algorithm is based on the 'shooting' principle described for instance in Atolia & Buffie (2009).[14] This amounts to guessing the initial values for consumption and resource prices and adjusting them until a stable solution consistent with the transversality condition (20) and resource constraints (23) is found. The following sequential structure illustrates our computational algorithm for an iteration of the model of length $t^{\max} > 0$.

---

[14] For a survey of applicable numerical procedures and advantages and drawbacks of forward-shooting algorithms see Judd (1992) and Trimborn, Koch & Steger (2008).

Step 1: Initialization for $t = 0$:[15]

    (a) Choose candidate initial values for consumption $\bar{C}_{-1} > 0$ and resource prices $(v_{1,-1}, v_{2,-1}) \in \prod_{i=1}^{2} [c_i, \infty[$. If $R_{i,0} = \infty$, set $v_{i,-1} = c_i$, otherwise $v_{i,-1} > c_i$.

    (b) Use these values together with the given parameters $\mathbf{S}_{-1} = (S_{1,-1}, S_{2,-1})$ and $\bar{K}_0 > 0$ to determine the endogenous part of θ_0. Set $t = 0$.

Step 2: Iteration for $0 \leq t \leq t^{\max}$:

    (a) Set up θ_t as in (A.6) using $\mathbf{N}_t^s$ and relevant endogenous variables from $t - 1$.

    (b) Compute ξ_t^1 by solving the problem $\Phi(\xi_t^1, \theta_t) = 0$ as outlined above.

    (c) Compute $\xi_t^2 = \Psi(\xi_t^1, \theta_t)$ as outlined above and check the following conditions:

        – If $\bar{K}_{t+1} < 0$, return to **Step 1** and decrease $\bar{C}_{-1}$.

        – If $\bar{C}_t < \bar{C}_t^{\mathrm{crit}}$, return to **Step 1** and increase $\bar{C}_{-1}$.

        – Otherwise, increase t by 1.

Step 3: Verification of resource constraints in $t = t^{\max}$:

    (a) For $i = 1, 2$ for which $R_{i,0} < \infty$, compute $R_{i,t^{\max}+1} := R_{i,0} - \sum_{t=0}^{t^{\max}} \sum_{\ell \in \mathbb{L}} X_{i,t}^{\ell}$:

        – If $R_{i,t^{\max}+1} < 0$, return to **Step 1** and increase $v_{-1,i}$.

        – If $R_{i,t^{\max}+1} > R_i^{\mathrm{crit}}$, return to **Step 1** and decrease $v_{-1,i}$.

    (b) If $0 < R_{i,t^{\max}+1} < R_i^{\mathrm{crit}}$ for all i for which $R_{i,0} < \infty$, complete the iteration. ∎

Step 2(c) in this algorithm requires the specification of a (typically time-dependent) lower bound $\bar{C}_t^{\mathrm{crit}}$ for consumption in period t.[16] The condition $\bar{C}_t > \bar{C}_t^{\mathrm{crit}}$ for all t serves to exclude cases where consumption *implodes*, i.e., converges to zero. This case occurs when initial consumption $\bar{C}_{-1}$ is chosen too small. Conversely, if $\bar{C}_{-1}$ is chosen to large, consumption *explodes*, i.e., grows too fast relative to output. In this case, the condition $\bar{K}_{t+1} > 0$ for all t will eventually be violated. Excluding both cases determines a unique initial value $\bar{C}_{-1}$ for which the equilibrium dynamics are well defined and satisfy the transversality condition (20). These features are well-known for the neoclassical growth model in state space form which exhibits saddle-path stability requiring initial consumption to be chosen on the stable manifold of values converging to the steady state. This behavior carries over to the present more complicated model.

---

[15]Specifying initial values for $\mathbf{v}_{-1} = (v_{1,-1}, v_{2,-1})$ and $\bar{C}_{-1}$ and computing $\mathbf{v}_0 = (v_{1,0}, v_{2,0})$ and $\bar{C}_0$ using (10) and (19) allows us to cast all computations for $t = 0$ in the same form as for periods $t > 0$. The structure of equations (10) and (19) and the fact that the values $\mathbf{v}_{-1}$ and $\bar{C}_{-1}$ only affect $\mathbf{v}_0$ and $\bar{C}_0$ shows that this approach is mathematically equivalent to assigning initial values to $\mathbf{v}_0$ and $\bar{C}_0$ directly.

[16]Our simulations use $\bar{C}_t^{\mathrm{crit}} = \bar{c}^{\mathrm{crit}} \sum_{\ell \in \mathbb{L}} \left(Y_t^\ell - \sum_{i=1}^{2} c_i X_{i,t}^\ell \right)$ where $\bar{c}^{\mathrm{crit}} = 0.01$.

Our numerical approach determines the unique sustainable initial level $\bar{C}_{-1}$ such that $\bar{K}_{t+1} > 0$ and $\bar{C}_t > \bar{C}_t^{\text{crit}}$ for all $t \leq t^{\max} + t^{\text{ahead}}$ for some $N^{\text{ahead}} \geq 0$.[17]

The conditions evaluated in Step 3 concern the world resource constraints (23). Clearly, this condition becomes relevant only for resources $i \in \{1,2\}$ for which $R_{i,0} < \infty$. Suppose this is the case and define $R_{i,t+1} := R_{i,t} - \sum_{\ell \in \mathbb{L}} X_{i,t}^\ell$ as the world resource stock at the end of period t. For any candidate resource price $\hat{v}_{i,-1}$, the induced sequence $(\hat{R}_{i,t})_{t \geq 0}$ of world resource stocks is strictly decreasing and, therefore, converges to a unique limit $\hat{R}_{i,\infty}$ which is zero at equilibrium. In our simulations, we establish that the sequence $(\hat{R}_{i,t})_{t \geq 0}$ becomes approximately constant within the length of iteration such that $\hat{R}_{i,\infty}$ can be approximated by $\hat{R}_{i,t^{\max}+1}$. We keep adjusting the initial resource price $\hat{v}_{i,-1}$ until $\hat{R}_{i,t^{\max}+1}$ becomes approximately zero, increasing $\hat{v}_{i,-1}$ when $\hat{R}_{i,t^{\max}+1} < 0$ and decreasing $\hat{v}_{i,-1}$ when $\hat{R}_{i,t^{\max}+1} > 0$. The iteration stops when all terminal resource stocks are positive and less than a pre-specified critical value R_i^{crit} which is chosen close to zero. The current value $\hat{v}_{i,-1}$ then approximates the true initial resource price $v_{i,-1}$.

A.4   Computing the equilibrium production allocation

The key challenge in our algorithm is to determine a vector ξ_t^1 which solves the condition $\Phi(\xi_t^1, \theta_t) = 0$ in Step 2(b). In this section we show how this problem can be transformed into an equivalent fixed problem which turned out to have very convenient properties in our simulations. Let vector θ_t determining labor supply $(N_t^{\ell,s})_{\ell \in \mathbb{L}}$, previous resource prices $(v_{1,t-1}, v_{2,t-1})$, the previous climate state $(S_{1,t-1}, S_{2,t-1})$, and aggregate capital $\bar{K}_t$ be given. For the sake of clarity, we organize the argument in three steps I-III.

I. Fix arbitrary values for outputs $(\bar{Y}_t^\ell)_{\ell \in \mathbb{L}}$ and energy mixes $(\bar{\eta}_t^\ell)_{\ell \in \mathbb{L}}$. We determine the factor allocation

$$A_t^f := ((N_{i,t}^\ell)_{i \in \mathbb{I}_0}, (K_{i,t}^\ell)_{i \in \mathbb{I}_0}, (X_{1,t}^\ell, X_{2,t}^\ell))_{\ell \in \mathbb{L}} \tag{A.7}$$

consistent with the equilibrium conditions as follows:

---

[17]In fact, to reduce computation time, we choose initial consumption C_{-1} such that $\bar{C}_t > \bar{C}_t^{\text{crit}}$ and $\bar{K}_{t+1} > 0$ holds for all $0 \leq t \leq t^{\text{ahead}} = 25$. Then, in each future period $t > 0$, the value $\bar{C}_t$ delivered by the Euler equation (19) is (slightly) adjusted such that $\bar{C}_{t+n} > \bar{C}_{t+n}^{\text{crit}}$ and $\bar{K}_{t+n} > 0$ holds for all $0 \leq n \leq t^{\text{ahead}}$. Thus, in each period, we adjust consumption to ensure that the consumption-capital dynamics is stable over the next t^{ahead} periods. As these adjustments are small if t^{ahead} is chosen sufficiently large, our approach is equivalent to choosing initial consumption C_{-1} such that the dynamics is stable for all $t \leq t^{\max} + t^{\text{ahead}}$ but turned out to be computationally faster. In addition, one can successively increase the accuracy of the simulations by gradually increasing t^{ahead}.

(a) For each $\ell \in \mathbb{L}$, determine regional labor allocation $(N_{i,t}^{\ell})_{i \in \mathbb{I}_0}$ by solving

$$\frac{1 - \alpha_0 - \nu_0}{N_{0,t}^{\ell}} = \frac{\nu_0(1 - \alpha_1 - \nu_1)}{N_{1,t}^{\ell}}\bar{\eta}_{1,t}^{\ell} = \frac{\nu_0(1 - \alpha_2 - \nu_2)}{N_{2,t}^{\ell}}\bar{\eta}_{2,t}^{\ell} = \frac{\nu_0(1 - \alpha_3)}{N_{3,t}^{\ell}}\bar{\eta}_{3,t}^{\ell}$$

$$N_t^{\ell,s} = \sum_{i=0}^{3} N_{i,t}^{\ell}$$

which follow from (A.4a) and (21). This gives the following solution:

$$N_{i,t}^{\ell} = \frac{n_{i,t}^{\ell}}{\sum_{j=0}^{3} n_{j,t}^{\ell}} N_t^{\ell,s}, \quad i \in \mathbb{I}_0$$

where

$$\begin{aligned}
n_{0,t}^{\ell} &= 1 - \alpha_0 - \nu_0 \\
n_{1,t}^{\ell} &= \nu_0(1 - \alpha_1 - \nu_1)\bar{\eta}_{1,t}^{\ell} \\
n_{2,t}^{\ell} &= \nu_0(1 - \alpha_2 - \nu_2)\bar{\eta}_{2,t}^{\ell} \\
n_{3,t}^{\ell} &= \nu_0(1 - \alpha_3)\bar{\eta}_{3,t}^{\ell}.
\end{aligned}$$

(b) Determine international capital allocation $((K_{i,t}^{\ell})_{i \in \mathbb{I}_0})_{\ell \in \mathbb{L}}$ by solving

$$\frac{\alpha_0}{K_{0,t}^{\ell}} = \frac{\nu_0\alpha_1}{K_{1,t}^{\ell}}\bar{\eta}_{1,t}^{\ell} = \frac{\nu_0\alpha_2}{K_{2,t}^{\ell}}\bar{\eta}_{2,t}^{\ell} = \frac{\nu_0\alpha_3}{K_{3,t}^{\ell}}\bar{\eta}_{3,t}^{\ell} \qquad \forall \ell \in \mathbb{L}$$

$$K_{0,t}^{\ell} = \frac{\bar{Y}_t^{\ell}}{\bar{Y}_t^1} K_{0,t}^1 \qquad \forall \ell \in \mathbb{L}$$

$$\bar{K}_t = \sum_{\ell \in \mathbb{L}} \sum_{i \in \mathbb{I}_0} K_{i,t}^{\ell}$$

which follow from (A.4b) and (22). This gives the following solution for $\ell \in \mathbb{L}$:

$$K_{i,t}^{\ell} = \frac{k_{i,t}^{\ell}}{\sum_{h \in \mathbb{L}} \sum_{j=0}^{3} k_{j,t}^{h}} \bar{K}_t, \quad i \in \mathbb{I}_0,$$

where

$$\begin{aligned}
k_{0,t}^{\ell} &= \alpha_0 \bar{Y}_t^{\ell} \\
k_{1,t}^{\ell} &= \nu_0\alpha_1 \bar{\eta}_{1,t}^{\ell} \bar{Y}_t^{\ell} \\
k_{2,t}^{\ell} &= \nu_0\alpha_2 \bar{\eta}_{2,t}^{\ell} \bar{Y}_t^{\ell} \\
k_{3,t}^{\ell} &= \nu_0\alpha_3 \bar{\eta}_{3,t}^{\ell} \bar{Y}_t^{\ell}.
\end{aligned}$$

(c) For each $\ell \in \mathbb{L}$, determine resource allocation $(X_{1,t}^{\ell}, X_{2,t}^{\ell})$ by solving

$$c_i + \frac{\alpha_0 \bar{Y}_t^1}{K_{0,t}^1}(v_{i,t-1} - c_i) + \zeta_i \bar{\tau} \sum_{h \in \mathbb{L}} \gamma^h \bar{Y}_t^h = \frac{\nu_0 \nu_i \bar{Y}_t^{\ell}}{X_{i,t}^{\ell}} \bar{\eta}_{i,t}^{\ell} \quad \text{for } i = 1, 2$$

which follows from (A.4c) and uses (A.4b) to replace r_t. This gives

$$X_{i,t}^\ell = \frac{\nu_0 \nu_i \bar{Y}_t^\ell \bar{\eta}_{i,t}^\ell}{c_i + \frac{\alpha_0 \bar{Y}_t^1}{K_{0,t}^1}(\nu_{i,t-1} - c_i) + \zeta_i \bar{\tau} \sum_{h \in \mathbb{L}} \gamma^h \bar{Y}_t^h} \qquad \text{for } i = 1, 2.$$

This first step defines a first mapping

$$G : (\bar{Y}_t^\ell, \bar{\eta}_t^\ell)_{\ell \in \mathbb{L}} \longmapsto A_t^f = ((N_{i,t}^\ell)_{i \in \mathbb{I}_0}, (K_{i,t}^\ell)_{i \in \mathbb{I}_0}, (X_{1,t}^\ell, X_{2,t}^\ell))_{\ell \in \mathbb{L}} \qquad \text{(A.8)}$$

determining factor allocation A_t^f from given outputs and energy mixes.

II. Use factor allocation A_t^f from (A.7) to recursively determine following variables:

   (a) Emissions Z_t and climate variables $S_{1,t}, S_{2,t}$ and S_t using (12) and (13)

   (b) Energy outputs $(E_{i,t}^\ell)_{i \in \mathbb{I}}$ and E_t^ℓ for each $\ell \in \mathbb{L}$ using (4), (7), and (2)

   (c) Final output Y_t^ℓ and energy mix η_t^ℓ for each $\ell \in \mathbb{L}$ from (1) and (A.3).

This second step defines a second mapping[18]

$$H : A_t^f = ((N_{i,t}^\ell)_{i \in \mathbb{I}_0}, (K_{i,t}^\ell)_{i \in \mathbb{I}_0}, (X_{1,t}^\ell, X_{2,t}^\ell))_{\ell \in \mathbb{L}} \longmapsto (Y_t^\ell, \eta_t^\ell)_{\ell \in \mathbb{L}} \qquad \text{(A.9)}$$

determining output and energy mixes from factor allocation and pre-determined variables.

III. The composition of the mappings (A.8) and (A.9)

$$F := H \circ G : (\bar{Y}_t^\ell, \bar{\eta}_t^\ell)_{\ell \in \mathbb{L}} \longmapsto (Y_t^\ell, \eta_t^\ell)_{\ell \in \mathbb{L}} \qquad \text{(A.10)}$$

maps the original variables $(\bar{Y}_t^\ell, \bar{\eta}_t^\ell)_{\ell \in \mathbb{L}}$ to a new value $(Y_t^\ell, \eta_t^\ell)_{\ell \in \mathbb{L}}$. It follows that the equilibrium solution $(Y_t^{\ell*}, \eta_t^{\ell*})_{\ell \in \mathbb{L}}$ is a fixed point of F in the $3L$-dimensional set $(\mathbb{R}_{++} \times \Delta_+^3)^L$. Hence, the problem of determining the equilibrium factor allocation in period t from pre-determined variables is equivalent to solving the previous $3L$-dimensional fixed point problem.

Our numerical simulations indicate that the fixed point $(Y_t^{\ell*}, \eta_t^{\ell*})_{\ell \in \mathbb{L}}$ is in fact globally stable such that simply iterating the function F starting with some arbitrary initial guess yields the desired result. Once the fixed point $(Y_t^{\ell*}, \eta_t^{\ell*})_{\ell \in \mathbb{L}}$ is found, the full factor allocation follows from $A_t^{f*} = G((Y_t^{\ell*}, \eta_t^{\ell*})_{\ell \in \mathbb{L}})$. The associated factor prices $(w_t^{\ell*})_{\ell \in \mathbb{L}}$ and r_t^* then follow directly by using A_t^{f*} in (A.4a) and (A.4b) which completes the vector ξ_t^1.

---

[18]Note that, in general, the map H in (A.9) does **not** split into independent component mappings H^ℓ : $((N_{i,t}^\ell)_{i \in \mathbb{I}_0}, (K_{i,t}^\ell)_{i \in \mathbb{I}_0}, (X_{1,t}^\ell, X_{2,t}^\ell)) \longmapsto (Y_t^\ell, \eta_t^\ell)$ for each $\ell \in \mathbb{L}$ due to the joint impact of the resource allocation $(X_{1,t}^\ell, X_{2,t}^\ell)_{\ell \in \mathbb{L}}$ on emissions and climate damages.

A.5 Regional consumption and transfers

The aggregate equilibrium (26) computed in the previous sections does not specify regional consumption $\mathbf{C}_t = (C_t^\ell)_{\ell \in \mathbb{L}}$ and the transfers (25) between regions. Computation of these values requires the specification of a transfer policy $\theta = (\theta^\ell)_{\ell \in \mathbb{L}}$ and the initial distribution of capital $(K_0^\ell)_{\ell \in \mathbb{L}}$ and exhaustible resources $(R_{i,0}^\ell)_{\ell \in \mathbb{L}}$ of both types $i = 1, 2$. Once these objects are specified, we need to approximate lifetime labor incomes $(W^\ell)_{\ell \in \mathbb{L}}$ and transfer incomes $(T^\ell)_{\ell \in \mathbb{L}}$ defined as above. For each $\ell \in \mathbb{L}$, define for $N \geq 0$

$$W_N^\ell := \sum_{t=0}^{N} q_t w_t^\ell N_t^\ell \tag{A.11}$$

and total discounted tax revenue

$$T_N := \sum_{t=0}^{N} q_t \tau_t \sum_{\ell \in \mathbb{L}} \left(\zeta_1 X_{1,t}^\ell + \zeta_2 X_{2,t}^\ell \right). \tag{A.12}$$

Both sequences $(W_N^\ell)_{N \geq 0}$ and $(T_N)_{N \geq 0}$ are strictly increasing and we verify numerically that they converge sufficiently fast and become nearly constant as $N \to t^{\max}$ where we use $t_{\max} = 50$. This allows us to approximate W^ℓ by $\hat{W}^\ell := W_{t^{\max}}^\ell$ and T^ℓ by $\hat{T}^\ell := \theta^\ell T_{t^{\max}}$. With these approximations, one can employ (18) to obtain (approximated) consumption in region $\ell \in \mathbb{L}$ as

$$\hat{C}_t^\ell = \hat{\mu}^\ell \bar{C}_t = \frac{r_0 K_0^\ell + \hat{W}^\ell + \Pi^\ell + \hat{T}^\ell}{\sum_{k \in \mathbb{L}} \left(r_0 K_0^k + \hat{W}^k + \Pi^k + \hat{T}^k \right)} \bar{C}_t \quad \text{for } t = 0, 1, 2, \ldots \tag{A.13}$$

with profit incomes Π^ℓ determined by (15). The latter is obtained from the distribution of (proven and estimated) reserves of oil and gas from Table 16 to which we add the consumption of oil/gas from Table 2 to obtain resource stocks at the beginning of $t = 0$.

B Data and Calibration Details

This section describes our data sources and how we transformed them to construct the main calibration targets in Table 2.

B.1 Details on regional structure

Our regional structure makes use of the world income classification from the World Bank (2018b). Specifically, we use their definition of 'high income', 'low income', and 'lower middle income' countries. Region 1 is the United States. Region 2 represents all of OECD-Europe. Region 3 comprises all 'high income' countries not contained in regions 1 or 2. Region 4 is mainland China. Region 6 contains all 'low income' and 'lower middle income' countries. Region 5 comprises the rest of the world.

B.2 Main calibration targets

B.2.1 Population data

We used population data and predictions from the 'Population Projection 2300' provided by the United Nations (2004).

B.2.2 Regional GDP

We use annual regional PPP-adjusted GDP data expressed in current international \$ from the World Bank (2018b). These values are aggregated over different countries based on our regional distinction and years 2006-2015.

B.2.3 Regional consumption of fossil fuels and emissions

We use data on regional primary energy demand from the IEA Energy Balances (2019) expressed in Gt of oil equivalents (oe). To convert coal consumption into metric giga tons (Gt), we use region-specific conversion factors which account for differences in types (hard coal and lignite) and quality (anthracite, subbituminous, and other bituminous) of coal. For hard coal, the conversion factor is 1.8 which is used for regions 4 and 5 where hard coal is the dominant type. Regions 1, 2, and 3 use high-quality hard coal but also a significant share of lignite for which the conversion factor is 3.4. For this reason, we use a higher factor of 2.0 for these regions. For region 6 we use an even higher factor of 2.2 because these countries typically use a large share of low-quality hard coal with lower energy content.

B.3 Climate damages

There is a great deal of uncertainty involved in predicting regional and global climate damages (see Section 3.3 in Hassler, Krusell & Smith (2016) for a detailed discussion). Hassler et al. (2020) (HKOR) use the projected regional damages from the 2010 version of the RICE-model associated with a 3.5 °C increase in temperature. Following table lists the damage values and parameters for the regions used in their study. Note that their damage function is identical to the one used in this paper.

Our approach here is to update these choices base on more recent evidence from the OECD (2015) and Burke et al. (2015). The OECD study provides estimates of regional GDP losses in 2060 under a hypothetical temperature increase of 2.6 °C. The projected values are reported in Table 14. Since the underlying temperature increase is smaller than the one consider in HKOR, the absolute damages are not directly comparable to Table 13.

Table 13: Regional damage parameters and climate damages from HKOR

	USA	EUR[1]	OCA[2]	CHN	IND[3]	SAM[4]	AFR[5]
GDP loss (+3.5 °C)	1.7%	1.9%	2.0%	1.8%	3.6%	1.8%	3.6%
$\gamma^\ell \cdot 10^5$	2.40	2.70	2.74	2.51	5.06	2.57	5.03

[1] Unlike our classification, this region represents all of Europe.

[2] This region referred to as 'Oceana' comprises most developed countries including Australia, Japan, Indonesia, Malaysia, Myanmar, New Zeeland, Phillipines, Thailand, and Vietnam.

[3] This region comprises India, Pakistan, and Bangladesh. [4] South America. [5] Africa.

Table 14: Regional GDP loss due to a temperature increase of 2.6 C°

Scenario	OECD Europe	OECD Pacific	OECD America	Latin America
Central projection	-0.2%	-0.3%	-0.6%	-1.5%
Upper bound	-0.3%	-0.3%	-0.6%	-1.6%
Lower bound	-0.1%	-0.1%	-0.3%	-0.8%
Scenario	Rest of Europe	Asia Middle East & North Africa	South and South-East Asia	Sub Saharan Africa
Central projection	-2.1%	-3.3%	-3.7%	-3.8%
Upper bound	-2.3%	-3.5%	-4.9%	-4.1%
Lower bound	-1.0%	-1.6%	-1.7%	-1.9%

Source: OECD (2015).

What we infer from Table 14 are the following features. First, climate damages in the US are two to three times larger than in OECD Europe. Second, climate damages in other developed countries (here represented by OECD Pacific) also tend to be lower than in the U.S. and are about the same as in OECD Europe. Third, climate damages for developing (Non-OECD Europe) and low income (Sub Saharan Africa, South and South-East Asia) countries are much higher and also much more uncertain than for industrialized countries. These findings are all in line with recent research by Burke et al. (2015) who predict much higher climate damages than previous IAM models which are, in addition, heavily biased towards low income and developing countries.

Based on this additional evidence, we mostly retain the damage prediction from HKOR for Europe but update the relative size of damages for the other regions based on the finding from Table 14. Since China is not included explicitly in OECD data, we follow HKOR by assuming that damages in China are about the same as in the U.S., a feature also in line with Burke et al.(2015).

Following Table 15 lists the percentage damages assumed in our calibration for the same temperature scenario as HKOR. To infer the damage parameters from the percentage GDP losses in Table 15, we adopt the calibration strategy devised by GHKT. First, we use temperature equation (33) to infer the stock of carbon S associated with the assumed increase of 3.5 °C in temperature. This gives a value of $S = 1304.5$ GtC. In

Table 15: Regional GDP loss due to a temperature increase of 3.5 C°

	USA	OEU	OHI	CHN	DEC	LIC
GDP loss in %	2.9%	1.5%	1.5%	2.9%	4.4%	5.8%
$10^5 \gamma^\ell$	4.12	2.05	2.05	4.12	6.22	8.33

a second step, we use this value in our damage function to compute the parameters γ^ℓ associated with the projected loss D^ℓ in regional GDP. This gives the inverse relation

$$\gamma^\ell = -\log(1 - D^\ell)/(S - \bar{S}) \tag{A.14}$$

where $S = 1304.5$ and $\bar{S} = 581$ as the pre-industrial stock of carbon. The damage parameters $(\gamma^\ell)_{\ell=1,..,6}$ inferred from (A.14) are also listed in Table 15.

B.4 Resource stocks

We distinguish 'proven reserves' defined as confirmed resource stocks of known size that can be extracted with currently available technologies and 'estimated reserves' referring to resource stocks of uncertain size and not profitable to extract with the available technologies. Based on this distinction, Table 16 displays empirical stocks of oil and gas for each region. The data is taken from BP Statistical Review (2018) and Federal Institute for Geosciences and Natural Resources Germany (2015).

Table 16: Regional stocks of fossil fuels in 2015 in Gt

	USA	OEU	OHI	CHN	DEC	LIC	World
			Proven reserves				
Oil	6.80	2.05	97.32	3.49	122.93	10.60	243.19
Natural gas[1]	6.87	2.53	35.05	4.12	86.62	15.63	150.83
Total Oil & Gas	13.67	4.58	132.36	7.62	209.56	26.23	**394.02**
Coal	253.74	82.29	165.93	140.91	209.74	213.92	**1066.54**
			Estimated reserves				
Oil	117.72	10.30	81.39	28.99	171.12	38.43	447.95
Natural gas[1]	40.37	14.55	82.43	48.06	236.29	54.12	475.81
Total Oil & Gas	158.09	24.85	163.81	77.05	407.41	92.55	**923.76**
Coal	7930.65	743.10	2308.93	5736.00	4718.70	978.55	**22415.94**

[1] Natural gas is given in tons of oil equivalent.

B.5 Resource prices and extraction costs

Table 17 shows empirical prices based on data from Worldbank (2018). Original prices of oil are reported in \$/bbl which we multiply by 7.14 to obtain prices in \$/t. Natural

gas prices originally given in $/mmbtu are multiplied by 1/0.02519 to obtain prices in $/t. Our calibration target 403.3 $/t is the weighted mean of these prices. Using Table 16 we determine the weight for oil as the share of proven and estimated oil reserves (691.14 Gt) relative to total proven and estimated oil and gas reserves (1317.8 Gt).

Table 17: Prices for crude oil and natural gas 2006-2015 in $/t[*]

	2006	2007	2008	2009	2010	2011	2012	2013	2014	2015	Average
Crude oil	459.0	507.8	692.5	440.9	564.4	742.6	749.8	743.1	687.1	362.4	595.0
Natural gas	266.8	277.2	351.6	156.8	174.1	158.7	109.3	148.0	173.5	103.8	192.0
Weighted mean	367.6	398.1	530.4	305.8	378.8	465.0	445.2	460.1	442.9	239.0	**403.3**

Source: Worldbank Global economic monitor commodities (2018).
[*] Nominal in current US-$.

B.6 U.S. energy data

Following table reports key U.S. energy statistics which were used in Section to calibrate key production parameters. U.S. physical energy demand is reported in Inter-

Table 18: U.S. Energy statistics 2006-2015

	2006	2007	2008	2009	2010	2011	2012	2013	2014	2015	2006-15
Final energy demand [Gtoe]											
Oil & Gas	1.21	1.22	1.17	1.12	1.16	1.13	1.12	1.15	1.17	1.18	**11.634**
Coal	0.19	0.20	0.19	0.17	0.18	0.17	0.15	0.15	0.15	0.13	**1.685**
Clean	0.15	0.15	0.16	0.16	0.16	0.17	0.17	0.18	0.19	0.19	**1.694**
Nominal final energy expenditures [Bill. U.S.-$]											
Oil & Gas	861	924	1075	749	882	1059	1052	1056	1062	824	**9545.0**
Coal	200	209	225	204	217	208	183	194	199	169	**2008.5**
Clean	98	101	109	113	115	124	120	126	134	135	**1174.2**

Source: U.S.-Energy Information Administration (EIA), International Energy Agency (IEA).

national Energy Agency (2019). Data for nominal energy expenditures are based on U.S.-Energy Information Administration (2019). To get nominal energy expenditures in bill. $ for each of our three energy sources, we used nominal expenditures for coal, oil and gas and clean energy for non-electric energy and added corresponding nominal expenditures for electricity. To get the latter, we computed %-shares in physical electricity production for each energy source and multyplied these shares with total nominal electricity retail sales.

B.7 Energy elasticities and aggregation parameters

First, we note from the third condition in (3) that $\sum_{i=1}^{3} p_{i,t}^{\ell} E_{i,t}^{\ell} = \nu_0 Y_t^{\ell}$. Using the values for nominal energy consumption from Table 18 and U.S. output from Table 2 (all expressed in trillion U.S.\$) permits to back out the energy elasticity in (1) as

$$\nu_0 = \bar{\nu}_0 := \frac{\sum_{i=1}^{3} \bar{E}_{i,0}^{1,\text{nom}}}{\bar{Y}_0^1} = \frac{9.545 + 2.008 + 1.174}{156.7} = \frac{12.728}{156.7} = 0.0812. \qquad (A.15)$$

Note this value is higher than the 4% used in GHKT, which seems quite plausible since we consider secondary energy products like electricity, heat, and transportation while GHKT consider primary energy inputs.

Second, we use the third optimality conditions in (3) to obtain the following ratios

$$\frac{\kappa_1}{\kappa_2} = \left(\frac{E_{1,t}^{\ell}}{E_{2,t}^{\ell}}\right)^{-\bar{\varrho}} \frac{p_{1,t}^{\ell} E_{1,t}^{\ell}}{p_{2,t}^{\ell} E_{2,t}^{\ell}} \quad \text{and} \quad \frac{\kappa_1}{\kappa_3} = \left(\frac{E_{1,t}^{\ell}}{E_{3,t}^{\ell}}\right)^{-\bar{\varrho}} \frac{p_{1,t}^{\ell} E_{1,t}^{\ell}}{p_{3,t}^{\ell} E_{3,t}^{\ell}}.$$

Inserting our observations for physical and nominal energy consumption in period $t = 0$ and region $\ell = 1$ using our pre-determined choice $\bar{\varrho} = 0.5$ gives

$$\frac{\kappa_1}{\kappa_2} = \left(\frac{11.634}{1.685}\right)^{-0.5} \frac{9.545}{2.008} = 1.809038 \quad \text{and} \quad \frac{\kappa_1}{\kappa_3} = \left(\frac{11.634}{1.694}\right)^{-0.5} \frac{9.545}{1.1742} = 1.510145. \qquad (A.16)$$

Solving these conditions using $\sum_{i=1}^{3} \kappa_i = 1$ yields $\kappa_1 = 0.53325$ and $\kappa_2 = 0.29483$.

Finally, we can write the equilibrium condition (6) in the laissez-faire case $\tau_t = 0$ as

$$\nu_i = \frac{v_{i,t} X_{i,t}^{\ell}}{p_{i,t}^{\ell} E_{i,t}^{\ell}} \quad \text{for } i = 1, 2. \qquad (A.17)$$

Inserting for $i = 1, 2$ our observations for nominal energy demand $\bar{E}_{i,0}^{1,\text{nom}}$ in billion U.S. \$ and resource extractions $\bar{X}_{i,0}^1$ in Gt from Table 2 for the U.S. economy together with the targets for exhaustible resource prices $\bar{v}_{i,0}$ in U.S. \$/t described above gives

$$\nu_1 = \bar{\nu}_1 = \frac{403.3 \cdot 13.9}{9545} = 0.5873 \quad \text{and} \quad \nu_2 = \bar{\nu}_2 = \frac{43 \cdot 9.6}{2008} = 0.2056. \qquad (A.18)$$

B.8 Determining productivity parameters Q_i^{ℓ}

Having determined $\nu_0 = \bar{\nu}_0$ by (A.15) and $\nu_i = \bar{\nu}_i$ by (A.18) for both $i = 1, 2$, we can use (A.17) in combination with the targets for global resource prices $\bar{v}_0^i$ and regional fossil fuel consumption $\bar{X}_{i,0}^{\ell}$ in $t = 0$ to back out nominal energy production in region ℓ as

$$E_{i,0}^{\ell,\text{nom}} = \bar{E}_{i,0}^{\ell,\text{nom}} := \bar{v}_{i,0} \bar{X}_{i,0}^{\ell} / \bar{\nu}_i \quad \text{for } i = 1, 2. \qquad (A.19)$$

Since we know from the third condition in (3) that $\sum_{i=1}^{3} \bar{E}_{i,0}^{\ell,\text{nom}} = \bar{v}_0 \bar{Y}_0^{\ell}$, we can use (A.19) to determine the full energy mix $\eta_0^{\ell} = \bar{\eta}_0^{\ell}$ defined in (A.2) for region ℓ as

$$\eta_{i,0}^{\ell} = \bar{\eta}_{i,0}^{\ell} := \bar{E}_{i,0}^{\ell,\text{nom}} / (\bar{v}_0 \bar{Y}_0^{\ell}) \quad \text{for } i = 1, 2, \quad \text{and} \quad \eta_{3,0}^{\ell} = \bar{\eta}_{3,0}^{\ell} := 1 - \bar{\eta}_{1,0}^{\ell} - \bar{\eta}_{2,0}^{\ell}. \quad \text{(A.20)}$$

Knowing the complete list of regional outputs and energy mixes $(\bar{Y}_0^{\ell}, \bar{\eta}_0^{\ell})_{\ell \in \mathbb{L}}$, we can determine the associated equilibrium factor allocation of capital and labor as in Step I of the algorithm described in Section A.4. Note that all equations involved in this step are independent of the Q_i^{ℓ}'s and the pre-determined variables are given by our initial values for aggregate capital $\bar{K}_0$ and labor supply $(\bar{N}_0^{\ell,s})_{\ell \in \mathbb{L}}$. This and the calibration targets for fossil fuel consumption $(\bar{X}_{i,0}^{\ell})_{i=1,2}$ for each region ℓ uniquely determine the initial factor allocation consistent with our calibration targets as

$$A_0^f = \bar{A}_0^f := ((\bar{N}_{i,0}^{\ell})_{i \in \mathbb{I}_0}, (\bar{K}_{i,0}^{\ell})_{i \in \mathbb{I}_0}, (\bar{X}_{1,0}^{\ell}, \bar{X}_{2,0}^{\ell}))_{\ell \in \mathbb{L}}. \quad \text{(A.21)}$$

Further, the target values for regional fossil fuel consumption determine global emissions $Z_0 = \bar{Z}_0$ by means of equation (12). Using these emissions and the given initial climate state $\bar{\mathbf{S}}_{-1} = (\bar{S}_{1,-1}, \bar{S}_{2,-1})$ in equation (13) determines the new climate state $\bar{\mathbf{S}}_0 = (\bar{S}_{1,0}, \bar{S}_{2,0})$ and regional initial climate damages $(\bar{D}_0^{\ell})_{\ell \in \mathbb{L}}$ follow from equation (14). Given these quantities, we choose the total factor productivity parameters $Q_i^{\ell} = \bar{Q}_i^{\ell}$ in each region ℓ to make production outputs in all sectors $i = 0, 1, 2, 3$ consistent with the targets for output $\bar{Y}_0^{\ell}$ and energy mix $\bar{\eta}_0^{\ell}$. First, we use our pre-determined values for production output, factors, and damages in (1) to back out the energy aggregate

$$E_0^{\ell} = \bar{E}_0^{\ell} := \left[\frac{\bar{Y}_0^{\ell}}{(1 - \bar{D}^{\ell})(\bar{K}_{0,0}^{\ell})^{\bar{\alpha}_0}(\bar{N}_{0,t}^{\ell})^{1 - \bar{\alpha}_0 - \bar{v}_0}} \right]^{\frac{1}{\bar{v}_0}}. \quad \text{(A.22)}$$

Further, using (A.22) and our pre-determined energy mix in (A.3) permits to infer energy outputs in region ℓ as

$$E_{i,0}^{\ell} = \bar{E}_{i,0}^{\ell} = \bar{E}_0^{\ell} \left(\frac{\bar{\eta}_{i,0}^{\ell}}{\bar{\kappa}_i} \right)^{\frac{1}{\bar{\varrho}}} \quad \text{for } i = 1, 2, 3. \quad \text{(A.23)}$$

Using the determined values for energy outputs from (A.23) and the factor inputs from (A.21) in (4) and (4) we can solve for the unknown factor productivities to obtain

$$Q_1^{\ell} = \bar{Q}_1^{\ell} := \frac{\bar{E}_{1,0}^{\ell}}{(\bar{K}_{1,0}^{\ell})^{\bar{\alpha}_1}(\bar{N}_{1,0}^{\ell})^{1-\bar{\alpha}_1-\bar{v}_1}(\bar{X}_{1,0}^{\ell})^{\bar{v}_1}}$$

$$Q_2^{\ell} = \bar{Q}_2^{\ell} := \frac{\bar{E}_{2,0}^{\ell}}{(\bar{K}_{2,0}^{\ell})^{\bar{\alpha}_2}(\bar{N}_{2,0}^{\ell})^{1-\bar{\alpha}_2-\bar{v}_2}(\bar{X}_{2,0}^{\ell})^{\bar{v}_2}}$$

$$Q_3^{\ell} = \bar{Q}_3^{\ell} := \frac{\bar{E}_{3,0}^{\ell}}{(\bar{K}_{3,0}^{\ell})^{\bar{\alpha}_3}(\bar{N}_{3,0}^{\ell})^{1-\bar{\alpha}_3}}.$$

Finally, note from (A.23) that this calibration strategy only works for $\bar{\varrho} \neq 1$, which we need to assume for otherwise the energy mix would be constant.

B.9 Labor and productivity growth

Denote the time- and region-specific growth rates of population and productivity by $g_{n,t}^{\ell}$ and $g_{a,t}^{\ell}$ such that

$$n_t^{\ell} = (1 + g_{n,t}^{\ell})n_{t-1}^{\ell} \quad \text{and} \quad a_t^{\ell} = (1 + g_{a,t}^{\ell})a_{t-1}^{\ell} \quad \text{for all } t > 0. \tag{A.24}$$

Similar to Nordhaus & Boyer (2000), we assume that these growth rates evolve as

$$g_{n,t}^{\ell} = g_n^{\ell} e^{-\delta_n t} \quad \text{and} \quad g_{a,t}^{\ell} = \bar{g}_a + g_a^{\ell} e^{-\delta_a t} \quad \text{for all } t > 0. \tag{A.25}$$

Thus, population growth is asymptotically zero while long-term productivity growth $\bar{g}_a$ is identical for all regions. This parameter is set to zero in Nordhaus & Boyer (2000) which therefore abstracts from long-run growth. The values for δ_n and δ_a in (A.25) determine the speed of convergence to the long-run values. Our choices $\delta_n = 0.3$ and $\delta_a = 0.005$ ensure that convergence obtains within the first twenty iteration periods. Initial population sizes $(n_0^{\ell})_{\ell \in \mathbb{L}}$ are directly based on the observations from Table 2. The growth parameter g_n^{ℓ} in (A.25) is chosen to match the population forecasts in $t = 2200$ from Table 2. As for the productivity sequence $(a_t^{\ell})_{t \geq 0}$, we set $\bar{g}_a = 1.01^{10} - 1$ to obtain a long-run productivity growth rate of 1% p.a. Initial productivity a_0^1 in the U.S. is normalized to one and we set $a_0^2 = 0.7$ and $a_0^3 = 0.9$ for the other developed regions and $a_0^4 = 0.25$, $a_0^5 = 0.35$, and $a_0^6 = 0.125$ to broadly capture lower initial productivity in these regions.[19] In addition, we set $g_a^{\ell} = 0$ for developed countries $\ell \in \{1, 2, 3\}$ and $g_a^{\ell} = 0.01$ for developing regions $\ell \in \{4, 5, 6\}$. This choice ensures that total GDP in the second set of regions catches up with GDP in rich countries well before 2100, which is in line with empirical projections. Following table summarizes our parameter values.

Table 19: Regional population and productivity growth parameters

Parameter	USA	OEU	OHI	CHN	DEC	LIC
$\bar{g}_n^{\ell}$	0.00516	0.00582	-0.00058	0.00263	-0.00491	-0.01599
g_n^{ℓ}	0.11501	-0.07607	-0.00299	-0.05580	0.04901	0.25064
$\bar{g}_a$	0.10462	0.10462	0.10462	0.10462	0.10462	0.10462
g_a^{ℓ}	0.00000	0.00000	0.00000	0.01000	0.01000	0.01000

B.10 Regional wealth levels

We used data from the Credit Suisse Research Institute (2019) which provides detailed wealth estimates at the country level. Using their Table 2-4 from pages 55–94, we averaged the wealth levels from 2006 to 2015 for each of our regions to obtain the wealth levels and shares listed in the following table.

---

[19]Since total factor productivities Q_i^{ℓ} in (4) and (7) are adjusted to match final output and primary energy consumption, our choices for a_0^{ℓ} merely smooth the values in Table 5 but do not affect our results.

Table 20: Average regional wealth 2006-2015

		USA	OEU	OHI	CHN	DEC	LIC	World
Level	[trill. U.S.$]	60.23	78.91	48.20	24.74	24.18	2.70	238.96
Share	[%]	25.2	33.0	20.2	10.4	10.1	1.1	100.0

Our initial values for regional capital assets $(K_0^\ell)_{\ell \in \mathbb{L}}$ were then computed by multiplying the shares from the last row of Table 20 with the initial world capital stock $\bar{K}_0$.

References

ACEMOGLU, D., P. AGHION, L. BURSZTYN & D. HEMOUS (2012): "The Environment and Directed Technical Change", *American Economic Review*, 102(1), 131âĂŞ166.

ATOLIA, M. & E. F. BUFFIE (2009): "Reverse Shooting Made Easy: Automating the Search for the Global Nonlinear Saddle Path", *Computational Economics*, 34(3), 273–308.

BARRAGE, L. (2020): "Optimal Dynamic Carbon Taxes in a Climate-Economy Model with Distortionary Fiscal Policy", *Review of Economic Studies*, 87(1), 1–39.

BODEN, T., G. MARLAND & R. ANDRES (2010): "Global, Regional, and National Fossil-Fuel CO2 Emissions", Carbon Dioxide Information Analysis Center, Oak Ridge National Laboratory, U.S. Department of Energy, Oak Ridge Tenn., U.S.A.

BRITISH PETROLEUM COMPANY (2018): "BP statistical review of world energy.", London: British Petroleum Co.

BURKE, M., S. M. HSIANG & E. MIGUEL (2015): "Global non-linear effect of temperature on economic production", *Nature*, 527(7577), 235–239.

CAI, Y. & T. S. LONTZEK (2019): "The Social Cost of Carbon with Economic and Climate Risks", *Journal of Political Economy*, 127, 2684–2734.

CARRARO, C., J. EYCKMANS & M. FINUS (2006): "Optimal transfers and participation decisions in international environmental agreements", *The Review of International Organizations*, 1(4), 379–396.

CREDIT SUISSE RESEARCH INSTITUTE (2019): *Global Wealth Databook 2019*. Credit Suisse, Zurich, Switzerland.

DENNING, F. & J. EMMERLING (2017): "A Note on Optima with Negishi Weights", Working paper.

DIETZ, S. & F. VENMANS (2019): "Cumulative carbon emissions and economic policy: In search of general principles", *Journal of Environmental Economics and Management*, 96(5), 108–129.

EARTH SYSTEM RESEARCH LABORATORY (2016): "Trends in atmospheric Carbon Dioxide", https://www.esrl.noaa.gov/gmd/ccgg/trends/global.html#global_data.

EYCKMANS, J. & H. TULKENS (2003): "Simulating coalitionally stable burden sharing agreements for the climate change problem", *Resource and Energy Economics*, 25, 299–327.

FEDERAL INSTITUTE FOR GEOSCIENCES AND NATURAL RESOURCES (2015): "Energy Study 2015. Reserves, Resources and Availability of Energy Resources", http://www.bgr.bund.de/EN/Themen/Energie/Produkte/energy_study_2015_summary_en.html.

GERLAGH, R. & M. LISKI (2018): "Consistent climate policies", *Journal of the European Economic Association*, 16(1), 1–44.

GERMAIN, M., P. TOINT, H. TULKENS & A. DE ZEEUW (2003): "Transfers to sustain dynamic core-theoretic cooperation in international stock pollutant control", *Journal of Economic Dynamics and Control*, 28, 79–99.

GOLOSOV, M., J. HASSLER, P. KRUSELL & A. TSYVINSKI (2014): "Optimal Taxes on Fossil Fuel in General Equilibrium", *Econometrica*, 82(1), 41–88.

HAMBEL, C., H. KRAFT & E. SCHWARTZ (2021): "The social cost of carbon in a non-cooperative world", *Journal of International Economics*, 131, 103490.

HARSTAD, B. (2012a): "Buy Coal! A Case for Supply-Side Environmental Policy", *Journal of Political Economy*, 120(1), 77–115.

——— (2012b): "Climate Contracts: A Game of Emissions, Investments, Negotiations, and Renegotiations", *Review of Economic Studies*, 79, 1527–1557.

——— (2016): "The Dynamics of Climate Agreements", *Journal of the European Economic Association*, 14(3), 719–752.

HASSLER, J. & P. KRUSELL (2012): "Economics And Climate Change: Integrated Assessment In A Multi-Region World", *Journal of the European Economic Association*, 10(5), 974–1000.

HASSLER, J., P. KRUSELL, C. OLOVSSON & M. REITER (2020): "On the effectiveness of climate policies", Working paper, IIES, Stockholm University.

HASSLER, J., P. KRUSELL & A. A. SMITH (2016): "Environmental Macroeconomics", in *Handbook of Macroeconomics, 1st Edition, Chapter 24*, ed. by J. B. Taylor & H. Uhlig. Elsevier (North Holland Publishing Co.), Amsterdam.

HILLEBRAND, E. & M. HILLEBRAND (2019): "Optimal Climate Policies in a Dynamic Multi-Country Equilibrium Model", *Journal of Economic Theory*, 179, 200–239.

———— (2021): "Inducing Cooperation in a Multi-region Model of Climate Change", Working paper.

INTERNATIONAL ENERGY AGENCY (2007-2017): *Key World Energy Statistics 2007-2017*. OECD Publishing, Paris.

———— (2010): *World Energy Outlook 2010*. OECD Publishing, Paris.

———— (2019): "World Energy Balances 2019", .

IPCC (2015): "Climate Change 2014: Synthesis Report. Contribution of Working Groups I, II and III to the Fifth Assessment Report of the Intergovernmental Panel on Climate Change", Core Writing Team, R.K. Pachauri and L.A. Meyer (eds.)]. IPCC, Geneva, Switzerland, 151 pp. Fifth Assessment Report.

JUDD, K. L. (1992): "Projection methods for solving aggregate growth models", *Journal of Economic Theory*, 58(2), 410 – 452.

NASA (2018): "Global Land-Ocean Temperature Index", Discussion paper, NASA Goddard Institute for Space Studies.

NEGISHI, T. (1960): "Welfare Econmics and the Existence of an Equilibrium for a Competitive Economy", *Metroeconomica*, 12, 92–97.

NORDHAUS, W. & P. SZTORC (2013): "DICE 2013R: Introduction and User's Manual", Discussion paper, Website: dicemodel.net.

NORDHAUS, W. & Z. YANG (1996): "A Regional Dynamic General-Equilibrium Model of Alternative Climate-Change Strategies", *American Economic Review*, 86, 741–765.

NORDHAUS, W. D. (1991): "To slow or not to slow: the economics of the greenhouse effect", *Economic Journal*, 101, 920–937.

NORDHAUS, W. D. & J. BOYER (2000): *Warming the World: Economic Models of Global Warming*. MIT Press, MA.

OECD (2015): *The Economic Consequences of Climate Change*. OECD Publishing, Paris.

OECD, IEA & NEA (2015): *Projected Costs of Generating Electricity*. OECD Publishing, Paris.

PAPAGEORGIOU, C., M. SAAM & P. SCHULTE (2017): "Substitution between Clean and Dirty Energy Inputs: A Macroeconomic Perspective", *Review of Economics and Statistics*, 99(2), 281–290.

REZAI, A. & F. VAN DER PLOEG (2015): "Robustness of a simple rule for the social cost of carbon", *Economic Letters*, 132, 48–55.

SINN, H.-W. (2012): *The Green Paradox. A Supply-Side Approach to Global Warming*. The MIT Press, Cambridge, Massachusetts, and London, GB.

TRIMBORN, T., K.-J. KOCH & T. M. STEGER (2008): "Multidimensional Transitional Dynamics: A Simple Numerical Procedure", *Macroeconomic Dynamics*, 12(3), 301–319.

UNITED NATIONS FRAMEWORK CONVENTION ON CLIMATE CHANGE (2015): "Paris Agreement", https://unfccc.int/sites/default/files/english_paris_agreement.pdf.

U.S BUREAU OF ECONOMIC ANALYSIS (2007): "Input-Output Accounts Data", http://www.bea.gov/industry/io-annual.htm.

U.S. ENERGY INFORMATION ADMINISTRATION (2019): "Annual Energy Review", http://www.eia.gov/totalenergy/data/annual/index.cfm.

VAN DEN BIJGAART, I., R. GERLAGH & M. LISKI (2016): "A simple formula for the social cost of carbon", *Journal of Environmental Economics and Management*, 77, 75–94.

VAN VUUREN, D., K. VAN DER WIJST & S. E. A. MARSMAN (2020): "The costs of achieving climate targets and the sources of uncertainty", *Nature Climate Change*, in press.

WORLD BANK (2018a): "Global Economic Monitor (GEM) Commodities", http://databank.worldbank.org/data/databases/commodity-price-data.

———— (2018b): "World Development Indicators (WDI)", https://datacatalog.worldbank.org/dataset/world-development-indicators.